

## RESEARCH ARTICLE

# The effect of sterol structure upon clathrin-mediated and clathrin-independent endocytosis

JiHyun Kim<sup>1</sup>, Ashutosh Singh<sup>2,\*</sup>, Maurizio Del Poeta<sup>2</sup>, Deborah A. Brown<sup>1,‡</sup> and Erwin London<sup>1,‡</sup>

## ABSTRACT

Ordered lipid domains (rafts) in plasma membranes have been hypothesized to participate in endocytosis based on inhibition of endocytosis by removal or sequestration of cholesterol. To more carefully investigate the role of the sterol in endocytosis, we used a substitution strategy to replace cholesterol with sterols that show various raft-forming abilities and chemical structures. Both clathrin-mediated endocytosis of transferrin and clathrin-independent endocytosis of clustered placental alkaline phosphatase were measured. A subset of sterols reversibly inhibited both clathrin-dependent and clathrin-independent endocytosis. The ability of a sterol to support lipid raft formation was necessary for endocytosis. However, it was not sufficient, because a sterol lacking a 3 $\beta$ -OH group did not support endocytosis even though it had the ability to support ordered domain formation. Double bonds in the sterol rings and an aliphatic tail structure identical to that of cholesterol were neither necessary nor sufficient to support endocytosis. This study shows that substitution using a large number of sterols can define the role of sterol structure in cellular functions. Hypotheses for how sterol structure can similarly alter clathrin-dependent and clathrin-independent endocytosis are discussed.

**KEY WORDS:** Liquid-ordered state, Rafts, Cholesterol, Placental alkaline phosphatase, Transferrin

## INTRODUCTION

Lipid rafts are believed to be regions of cellular plasma membranes that contain tightly packed sphingolipids and sterols existing in the liquid ordered (Lo) state. They are thought to co-exist in the plasma membrane with liquid disordered (Ld) domains, which are rich in lipids that pack loosely because they have unsaturated acyl chains (Brown and London, 1997; Schroeder et al., 1994; Veatch and Keller, 2005). Although the existence of lipid rafts in the cell plasma membrane is still not universally accepted, very recent studies have provided strong evidence for their presence in mammalian cells (Kinoshita et al., 2017; Komura et al., 2016; Stone et al., 2017). Rafts have been proposed to be involved in many biological processes, including cellular viability, differentiation, infection, signaling pathways, and the sorting of membrane lipids and proteins (Bang et al., 2005; George et al., 2012; Gniadecki, 2004; Head et al., 2014; Xu et al., 2009).

Because sterol is crucial for Lo domain formation, disruption of domains by depletion of sterols using methyl- $\beta$ -cyclodextrin (M $\beta$ CD) or sequestration of sterols with nystatin or amphotericin B has been widely used to study the function of sterols in cells (Holz, 1974; Zidovetzki and Levitan, 2007). However, this is a very indirect way to test Lo domain function. It assumes that removing cholesterol destroys Lo domain formation, as demonstrated by a loss of detergent insolubility, a common property of ordered domains (Cermeus et al., 1993). However, ordered domains become more soluble in detergent at lower cholesterol concentrations, so loss of detergent insolubility does prove ordered domains have been lost (Brown, 2006; London, 2005; London and Brown, 2000; Schroeder et al., 1998). In addition, removal of cholesterol can have pleiotropic effects. Thus, cholesterol removal could indicate loss of a functionally important cholesterol–protein interaction, or could have an effect by altering the total amount of plasma membrane bilayer and its lipid:protein ratio (Monnaert et al., 2004; Ohtani et al., 1989).


As noted above, cholesterol supports ordered domain formation because of its ability to pack tightly with sphingolipids (Silvius, 2003; Xu and London, 2000). The structural features of cholesterol that have been suggested to be important for this are: flat fused rings, the small hydroxyl polar headgroup at C3, the isoocetyl alkyl tail attached at C17 and the small molecular area (Beattie et al., 2005; Wenz and Barrantes, 2003). These features are not shared by all sterols and steroids, and so sterols and steroids have a wide range of abilities to support or inhibit ordered domain formation (Beattie et al., 2005; Megha et al., 2006; Wang et al., 2004; Wenz and Barrantes, 2003; Xu and London, 2000). It is possible to alter sterol planarity, aliphatic side-chain properties, double bond locations and the presence of a polar 3-OH group.

By sterol substitution, sterol structure and membrane properties can be varied under conditions such that total membrane lipid is more-or-less constant. This raises the possibility that replacing membrane cholesterol with different sterols might define when ordered domains are involved in biological functions (Xu and London, 2000), and a number of such studies have been carried out (as recently reviewed Kim and London, 2015). There are several ways to alter membrane sterol without changing sterol levels. In several earlier studies, treatment with cholesterol oxidase (which converts cholesterol into 4-cholesten-3-one) or exchanging sterol with bovine serum albumin (BSA) or liposomes was used. However, the most widely used method has become exchange with M $\beta$ CD (Cheng et al., 2009; Gimpl et al., 1997; Huang and London, 2013; Romanenko et al., 2004). The ability of M $\beta$ CD to efficiently exchange a wide variety of sterols allows the widest possible variation of sterol structure. In some cases, function is strongly correlated with the ability to form ordered domains, while in other cases sterol dependence of function is not linked to the ability to form ordered domains (Brown et al., 2002; Campbell et al., 2004; Fahrenholz et al., 1995; Gimpl et al., 1997; Kalyana

<sup>1</sup>Dept. of Biochemistry and Cell Biology, Stony Brook University, Stony Brook, NY 11794, USA. <sup>2</sup>Dept. of Molecular Genetics and Microbiology, Stony Brook University, Stony Brook, NY 11794, USA.

\*Present address: Dept. of Biochemistry, University of Lucknow, Lucknow, Uttar Pradesh, India - 226007.

<sup>‡</sup>Authors for correspondence (Deborah.Brown@stonybrook.edu; Erwin.London@stonybrook.edu)

 A.S., 0000-0002-0995-6696; E.L., 0000-0002-1295-0113

Sundaram et al., 2016; Klein et al., 1995; LaRocca et al., 2010; Nimmo and Cross, 2003; Pang et al., 1999; Romanenko et al., 2004, 2009; Yamamoto et al., 2011).

Endocytosis, phagocytosis and other molecular trafficking events in cells are known to be affected by removal of cholesterol or sphingomyelin (SM), constituents of lipid rafts (Le et al., 2002; Pucadyil et al., 2004; Refaei et al., 2011; Shakor et al., 2011; Sharma et al., 2004; Subtil et al., 1999). Endocytosis can also be associated with a change in membrane order (Gaus et al., 2006). This suggests that endocytosis and related phenomena are regulated by lipid organization or raft domain formation in the plasma membrane.

To further investigate this, we studied two kinds of endocytosis: that of clustered placental alkaline phosphatase (PLAP, also known as ALPP) and of transferrin (TF). These proteins are endocytosed by different mechanisms (Mayor et al., 2014; Miaczynska and Stenmark, 2008). PLAP is a glycosylphosphatidylinositol (GPI)-anchored cell surface protein. GPI-anchored proteins are often relatively enriched in raft domains, especially when clustered (Baumgart et al., 2007; Paulick and Bertozzi, 2008; Schroeder et al., 1994). This is believed to be due to the saturated fatty acid chains attached to the GPI group (Schroeder et al., 1994; Maeda et al., 2007). GPI-anchored proteins are internalized from the cell surface by clathrin-independent endocytosis. This can occur via the clathrin-independent carriers (CLIC) and GPI-anchored protein-enriched compartments (GEEC) pathway, which is regulated by GRAF1 (also known as ARHGAP26) and Cdc42, and by a pathway regulated by Arf6 (Chadda et al., 2007; Diaz-Rohrer et al., 2014; Mayor et al., 2014; Miaczynska and Stenmark, 2008). GPI-anchored proteins can also be internalized via caveolae or a caveolae-like pathway, in a manner that is stimulated by antibody-mediated clustering (Parton et al., 1994). Binding of immunoglobulin G (IgG) to PLAP is a step in the transcytosis of the IgG molecule, which ultimately results in transfer of IgG from mother to fetus across the placental barrier (Kristoffersen, 2000; Makiya and Stigbrand, 1992). Endocytosis by all these clathrin-independent pathways requires cholesterol (Diaz-Rohrer et al., 2014; Mayor et al., 2014). However, the detailed mechanism of internalization in these cases is still undefined. Therefore, we examined the role of cholesterol structure and sterol lipid raft-forming properties in the endocytosis of clustered PLAP.

Clathrin-mediated endocytosis also requires cholesterol (Robinson, 2015; Subtil et al., 1999). However, partial depletion of cholesterol can inhibit clathrin-independent endocytosis without affecting the clathrin-dependent pathway, suggesting that the latter pathway is less sensitive to cholesterol level (Doherty and McMahon, 2009; Kirkham et al., 2005). Additionally, decreased clathrin-mediated endocytosis upon inhibition of SM synthesis has been shown (Shakor et al., 2011). It has been also reported that a cooperative effect of rafts and clathrin is involved in internalization of cellular prion protein (PrP<sub>c</sub>) (Sarnataro et al., 2009). Here, we studied endocytosis of the iron-carrier protein TF by the transferrin receptor (TFR), one of the best-characterized cargoes of clathrin-mediated endocytosis (Doherty and McMahon, 2009; Mayle et al., 2012; Robinson, 2015).

By performing sterol substitution, we find that endocytosis of both clustered PLAP and TF endocytosis have a similar dependence on the details of sterol structure, and that the effect of sterol substitution is reversible. It appears that both the ability of a sterol to support ordered domain formation and the presence of a sterol 3 $\beta$ -OH group are crucial. Hypotheses that might explain these observations are discussed.

## RESULTS

To define the effect of sterol structure upon endocytosis, cell sterol (note that although in a formal sense cholesterol analogs without an OH group are steroids not sterols, we will refer to all cholesterol analogs as sterols for simplicity) composition was altered by M $\beta$ CD-catalyzed sterol substitution. The sterols chosen had different structures at carbon 3, at which cholesterol has a 3 $\beta$ -OH group, different numbers and positions of double bonds, different degrees of ring planarity, different aliphatic tail structures, and a range of abilities to support or inhibit ordered domain formation (Beattie et al., 2005; Megha et al., 2006; Wang et al., 2004; Xu et al., 2001; Xu and London, 2000) (Fig. 1; Table S1).

### The effect of cholesterol amount upon PLAP and TF endocytosis

First, how endocytosis is affected by the amount of cholesterol in cells was determined. Cholesterol was depleted by incubating cells with M $\beta$ CD, and then the cells were replenished with cholesterol pre-loaded onto 2.5 mM M $\beta$ CD. Cholesterol levels were determined by using high-performance thin-layer chromatography (HP-TLC) (Fig. 2A). Depletion removed ~65% of cholesterol relative to that in untreated (control) cells (Fig. 2B; Table 1). After replenishment, cholesterol levels were restored to a degree dependent upon the amount of cholesterol loaded onto the M $\beta$ CD (Fig. 2B). Sterol-loading M $\beta$ CD using 0.1 mM cholesterol resulted in replenishment of cellular cholesterol to a level similar to that in untreated cells. Using 0.2 or 0.5 mM cholesterol loaded onto M $\beta$ CD cholesterol resulted in cholesterol levels about two-fold greater than in untreated cells.

Next, PLAP and TF endocytosis were measured in cholesterol-depleted or cholesterol-replenished cells. After induction of endocytosis, surface-bound anti-PLAP antibodies or surface-bound TF molecules were removed through an acid wash, and internalized antibody or TF fluorescence visualized in a confocal z-stack image of entire cells (Fig. 2C,E). Internalized Alexa Fluor 488 (AF488)-conjugated TF was easily quantified by measurement of total fluorescence after removing externally bound TF molecules. Integrated fluorescence intensity in a cell was measured, subtracting background fluorescence intensity to calculate corrected total cell fluorescence (CTCF). Internalized PLAP was distributed in distinct large puncta. We found that quantifying PLAP endocytosis from the puncta number:cell ratio was more sensitive and reproducible than measurements of total internalized anti-PLAP antibody fluorescence.

Both PLAP and TF endocytosis were affected by cholesterol level (Fig. 2D,F). Cholesterol levels lower than those in untreated cells inhibited endocytosis, with endocytosis gradually increasing as cholesterol amount was increased. PLAP endocytosis was restored to 50% of the level in untreated cell levels when the amount of cholesterol was restored to ~50% of that in the untreated cells, which corresponds to restoration of 25–40% of the removed cholesterol. TF endocytosis showed less sensitivity to cholesterol and was restored to ~50% of that in untreated cells when cholesterol levels were restored to ~40% of those in the untreated cells. Excess cholesterol, above that found in untreated cells, did not increase endocytosis above the level of that in untreated cells. A similar ability to control sterol level by substitution, and a similar dependence of PLAP and TF endocytosis upon sterol concentration, were observed for desmosterol (Fig. S1).

### Amount of sterols in cells after sterol substitution

To analyze the level of substitution of each sterol, HP-TLC or gas chromatography-mass spectrometry (GC-MS) were performed.

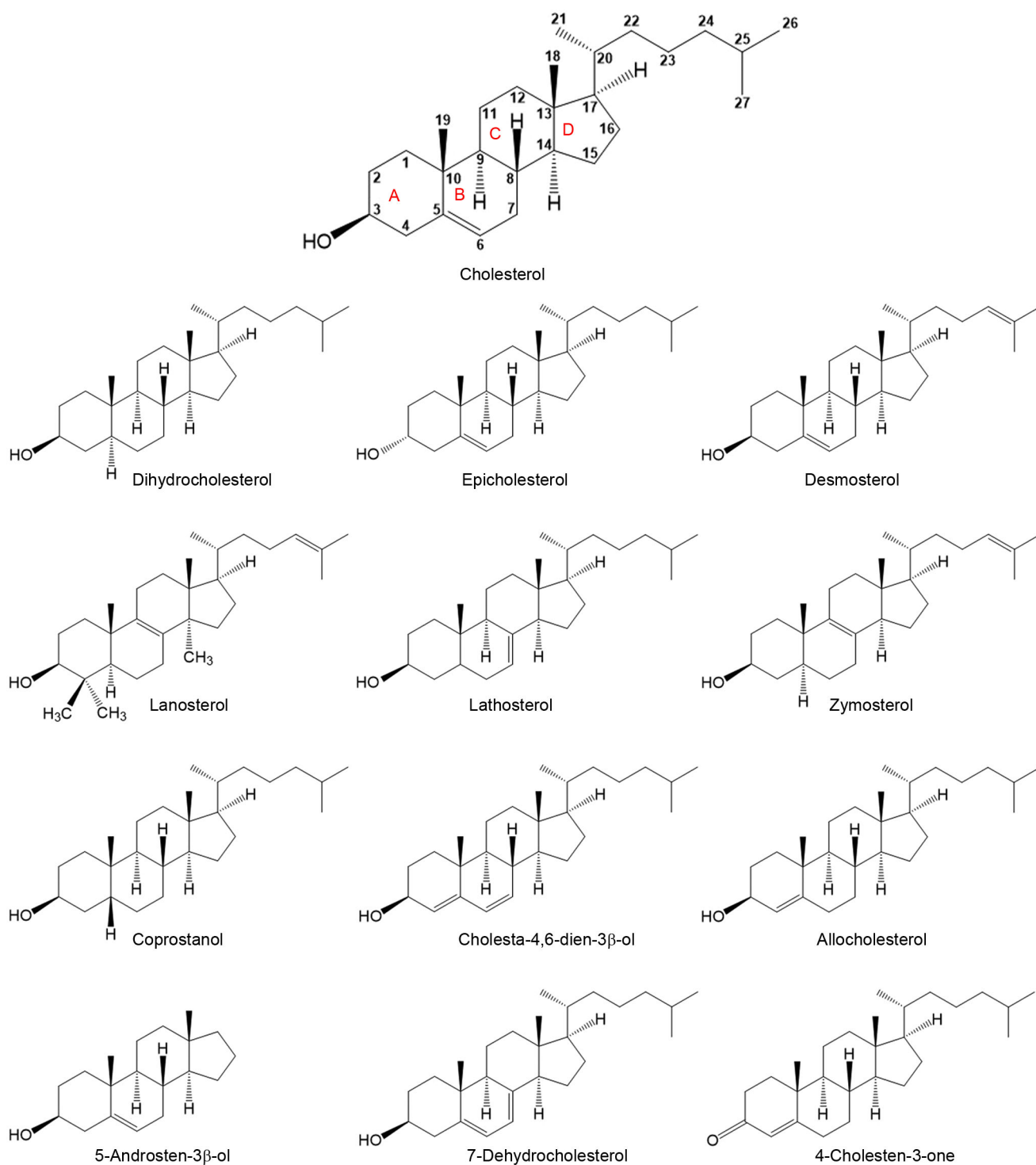


**Fig. 1. Structures of sterols used in this study.** Numbers in cholesterol structure indicates carbon number. A ring, carbon 1–5 and 10, B ring, carbon 5–10; C ring, carbon 8–9 and 11–14; and D ring, carbon 13–17.

After doing HP-TLC analysis of sterols from sterol-substituted cells, the sterol amount was quantified by measuring the band intensity and comparing to the levels for standard bands of the sterol, and then normalized to the amount of cellular protein (Table 1). The level of substitution varied significantly, with the amount of total sterol after substitution being 65–250% of the cholesterol in untreated cells. In most cases, the total sterol amount after substitution was similar to or higher than in untreated

cells. The exceptions were substitution with epicholesterol, lanosterol and lathosterol, which resulted in total sterol levels of about two-thirds of those in untreated cells. Because some sterols (desmosterol and dihydrocholesterol) have a similar mobility (retention factor=Rf) as cholesterol on HP-TLC, they were detected as a single band with cholesterol. Thus, only total sterol levels could be estimated for these sterols. However, it was confirmed that substitution efficiency was also substantial for

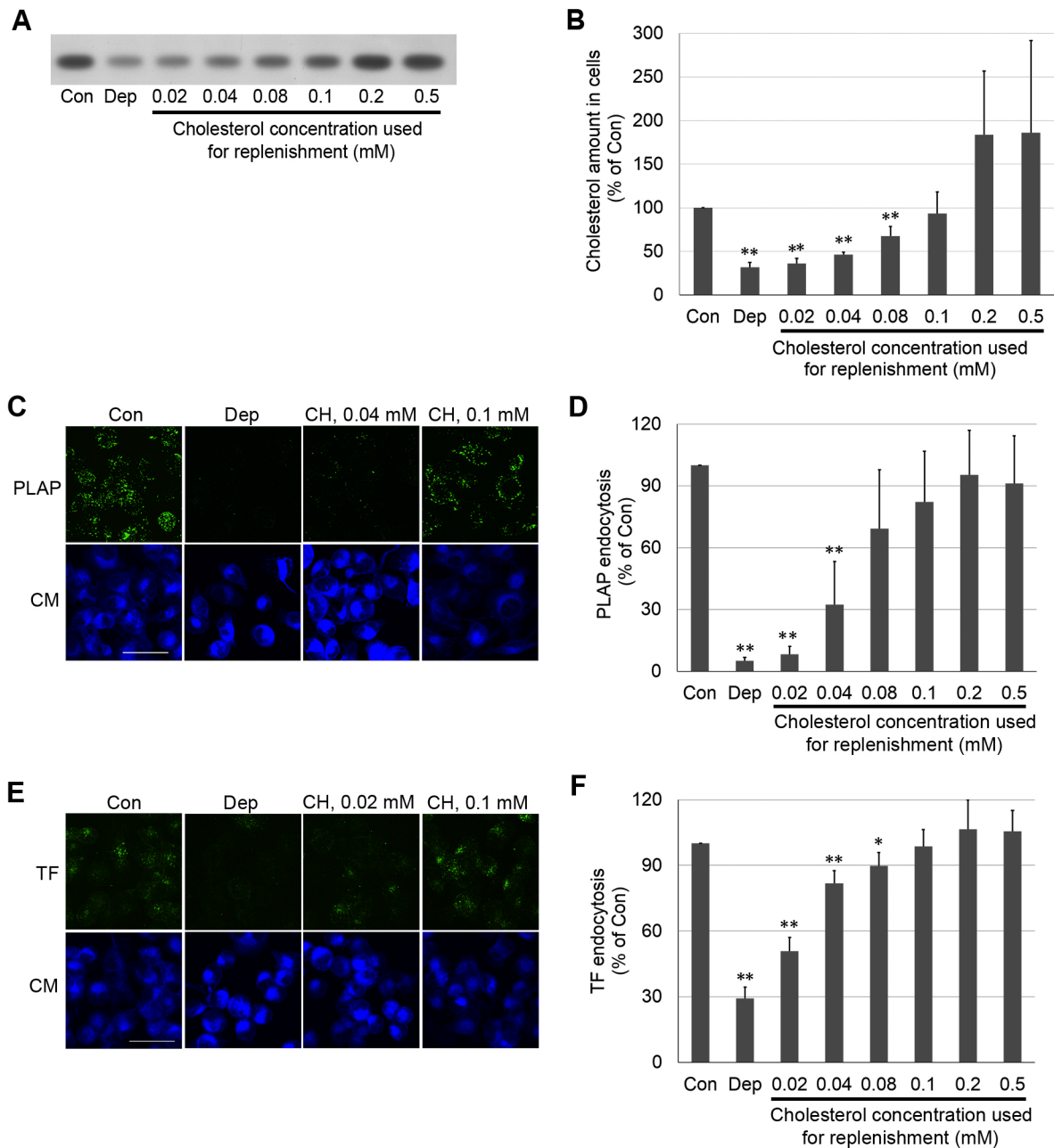


**Fig. 2. Both PLAP- and TF-endocytosis are regulated by cholesterol amount in cells.** (A) HP-TLC plate showing cholesterol amount in cells after cholesterol depletion (Dep) or replenishment. (B) Quantified cholesterol amounts determined from HP-TLC band intensity. (C) z-stack micrographs of PLAP endocytosis after cholesterol depletion or replenishment. After cholesterol depletion or replenishment, PLAP was clustered with antibody (green fluorescence), and clustered PLAP was internalized in a 20 min incubation at 37°C. Cell surface antibodies were removed by acid washing, and cell membranes were counter-stained with CellMask (CM, blue fluorescence). (D) Internalized PLAP puncta per cell. In each experiment 3–7 images (total cell number  $\geq 50$ ) were used for puncta quantitation. (E) z-stack micrographs of TF endocytosis after cholesterol depletion or replenishment. After cholesterol depletion or replenishment, TFRs on cell surface were bound with AF488–TF (green fluorescence) and allowed to endocytose in a 7 min incubation at 37°C. AF488–TF remaining on cell surface was removed by acid washing. Cell membranes were counter-stained with CellMask. (F) TF endocytosis in cells quantified from integrated fluorescence intensity. Endocytosis in 50 cells (2–3 images) was analyzed in each experiment. In B, D and F, the means.d. from three independent experiments are shown. Values normalized to untreated control cells. Con, untreated control cells; Dep, cholesterol-depleted cells; CH, cholesterol. Scale bars: 50  $\mu\text{m}$ . \* $P < 0.05$ ; \*\* $P < 0.01$  compared to 'Con' (unpaired, two-tailed Student's *t*-test).

these sterols by performing a GC-MS analysis, with desmosterol levels after substitution being 300% and dihydrocholesterol levels being  $\sim 115\%$  that of cholesterol in untreated cells (data not shown). It should be noted that GC-MS gave similar results to HP-TLC for most sterols, except for several sterols that appeared to degrade during GC-MS. However, we noticed that the GC-MS

results were generally more variable. After substitution, the amount of cholesterol, as assayed by HP-TLC or (not shown) GC-MS, generally decreased to values lower than that after just depleting cholesterol. In these cases, cholesterol levels were decreased to 15–25% of the control level, or even less in some cases, by sterol substitution.

**Table 1. Sterol substitution level as analyzed by HP-TLC**

	Cholesterol/ protein ( $\mu\text{g}/\text{mg}$ )	Substituted sterol/ protein ( $\mu\text{g}/\text{mg}$ )	Total sterol/ protein ( $\mu\text{g}/\text{mg}$ )
Untreated	19.7 $\pm$ 7.8	NA	19.7 $\pm$ 7.8
Cholesterol depletion	7.0 $\pm$ 3.7	NA	7.0 $\pm$ 3.7
Cholesterol replenishment	29.8 $\pm$ 19.6	NA	29.8 $\pm$ 19.6
4-cholesten-3-one	8.3 $\pm$ 6.3	13.9 $\pm$ 9.5	22.2 $\pm$ 11.4
5-androsten-3 $\beta$ -ol	5.5	35	40.5
7-dehydrocholesterol	2.4 $\pm$ 0.6	29.7 $\pm$ 1.5	32.1 $\pm$ 1.6
Allocholesterol	3.9 $\pm$ 0.5	18.1 $\pm$ 4.0	22 $\pm$ 4.0
Cholesta-4,6-dien- 3 $\beta$ -ol	5.0 $\pm$ 0.3	36.2 $\pm$ 9.0	41.2 $\pm$ 9.0
Coprostanol	3.7 $\pm$ 0.2	18.0 $\pm$ 4.6	21.7 $\pm$ 4.6
Desmosterol	NA	NA	53.1 $\pm$ 14.0
Dihydrocholesterol	NA	NA	31.0 $\pm$ 4.2
Epicholesterol	4.2 $\pm$ 0.4	9.2 $\pm$ 0.1	13.4 $\pm$ 0.4
Lanosterol	3.7 $\pm$ 0.6	9.7 $\pm$ 2.1	13.4 $\pm$ 2.2
Lathosterol	1.7 $\pm$ 0.1	12.6 $\pm$ 1.9	14.3 $\pm$ 1.9
Zymosterol	0.8 $\pm$ 0.2	49.7 $\pm$ 31.7	50.5 $\pm$ 31.7

Each sterol amount was quantitated from bands on TLC plates using ImageJ and SlideWrite programs. Mean $\pm$ s.d. are shown from independent experiments, with  $n=3$  except for untreated and cholesterol-depleted ( $n=20$ ), and 5-androsten-3 $\beta$ -ol ( $n=1$ ) samples. NA, not applicable.

### Effects of sterol substitution in cellular plasma membrane upon PLAP and TF endocytosis

Antibody-clustered PLAP and TF endocytosis was studied in sterol-substituted cells. The level of PLAP endocytosis was highly dependent upon sterol structure, with some sterols supporting endocytosis as well as cholesterol did, some inhibiting endocytosis to a level even greater than that after cholesterol depletion, and some sterols giving intermediate levels of endocytosis (Fig. 3A,B). The level of TF endocytosis was similarly affected by sterol type (Fig. 3C,D). Interestingly, the influence of sterols on the two types of endocytosis (PLAP and TF) was similar, with a strong correlation between their endocytosis levels ( $R^2=0.91$  for TF at 23°C and PLAP at 37°C). This correlation is lower ( $R^2=0.73$  at 37°C; Fig. 3E) when endocytosis of PLAP and TF endocytosis at 37°C are compared. This loss of correlation is an artifact of the fact that TF endocytosis is much faster at 37°C than at room temperature, as previous studies also noted (Hamilton, 1983; Rode et al., 1997; Tomoda et al., 1989). TF endocytosis is so fast at 37°C that a steady-state TF distribution between the surface and endocytic vesicles is rapidly established, suppressing sterol-dependent differences in the initial rate of TF endocytosis.

Some of the variation in endocytosis levels with different sterols could be due to different sterol levels after substitution. However, this does not explain the difference between cholesterol and other sterols. This can be seen by comparing the endocytosis levels after sterol substitution to that in cells with equivalent amounts of cholesterol (Fig. S2). For both PLAP and TF, cells in which cholesterol was replaced with desmosterol, 7-dehydrocholesterol, dihydrocholesterol and lathosterol supported 50–100% of the endocytosis levels (over the baseline for cholesterol-depleted cells) relative to cells having a comparable amount of cholesterol. Other sterols [coprostanol, 4-cholesten-3-one, epicholesterol, lanosterol, and 5-androsten-3 $\beta$ -ol (androstenol)] showed very low endocytosis levels relative to that with equivalent amounts of cholesterol, or did not even support endocytosis above baseline levels. A few sterols showed behavior dependent on the type of endocytosis or temperature. Substitution with cholesta-4,6-dien-3 $\beta$ -ol supported  $\sim 50\%$  (over baseline) as much PLAP endocytosis as an equivalent

amount of cholesterol, but only  $\sim 25\%$  as much TF endocytosis as an equivalent amount of cholesterol. Allocholesterol showed virtually no increase in endocytosis over baseline for both PLAP and TF, except in the case of TF endocytosis at 37°C. Zymosterol supported a low level of endocytosis over baseline for both PLAP ( $\sim 20\%$ ) and TF ( $\sim 25\text{--}40\%$ ). It should be noted that we also attempted to carry out substitution with the plant sterol sitosterol. Only low levels of substitution could be achieved, and substantial endocytosis (to a level even higher than that for cholesterol) was only noted for PLAP and only when we loaded M $\beta$ CD in the presence of a very high concentration of sitosterol (data not shown).

We were concerned that cholesterol depletion or substitution with another sterol could decrease the amount of PLAP or TF receptor (TFR) in the plasma membrane. This could reduce the level of endocytosis observed. To check this, the fluorescence of immunostained plasma membrane PLAP and TFR were measured immediately after cholesterol depletion, sterol substitution and fixation (Fig. 4). In the case of PLAP, only a small effect, at most, of sterol depletion or substitution upon plasma membrane PLAP levels were observed. Therefore, it appears that reduced plasma membrane localization of PLAP is unlikely to explain strong inhibition of PLAP endocytosis. In the case of TFR, sterols that inhibited endocytosis actually doubled the level of surface TFR. This also cannot explain reduced endocytosis. It is possible that in cases in which endocytosis was inhibited, the amount of inhibition would actually be greater than we measure by up to two-fold, if corrected for the extra receptor on the surface. The fact that the amount of TFR in plasma membrane increased upon cholesterol depletion or substitution with sterols that inhibit endocytosis (4-cholesten-3-one and allocholesterol) is consistent with a previous report showing that surface receptor levels increase upon cholesterol depletion (Subtil et al., 1999). It appears that interfering with TF endocytosis resulted in more TFRs being retained in the plasma membrane. This is consistent with a model in which endocytosis is blocked prior to any blockage of recycling (see Discussion).

We wanted to rule out the possibility that the loss of endocytosis upon sterol substitution was due to irreversible damage to the cells, or to some other irreversible change in cell properties. Reversibility was measured by first replacing cholesterol with a sterol that inhibits endocytosis, and then substituting cholesterol back into cells in a second substitution step. Fig. 5 shows that the inhibition of both endocytosis of PLAP and TF by sterol substitution was reversed by a second sterol substitution step using cholesterol. This demonstrates that the inhibition of endocytosis by sterol substitution does not involve an irreversible change in the cells.

The same type of experiments provided information about the localization of sterol (Fig. S3A). After sterol substitution, the degree to which a sterol is replaced with cholesterol in a second substitution step should largely reflect the degree to which it was localized in the plasma membrane, or at least cycles rapidly to the plasma membrane. When lanosterol was introduced into cells by substitution, it could be largely removed by a second round of exchange using cholesterol, suggestive of a plasma membrane localization for lanosterol, or at least that lanosterol recycles to the plasma membrane rapidly enough to be susceptible to exchange. Allocholesterol and 4-cholesten-3-one were found to be partially resistant to removal by a second round of exchange using cholesterol, even though substantial cholesterol was introduced into the cells. This may indicate that these sterols do not fully reside in the plasma membrane after exchange, although it is also possible that they are simply more difficult to remove in the second round of exchange. It is noteworthy that, for all of these sterols, the amount

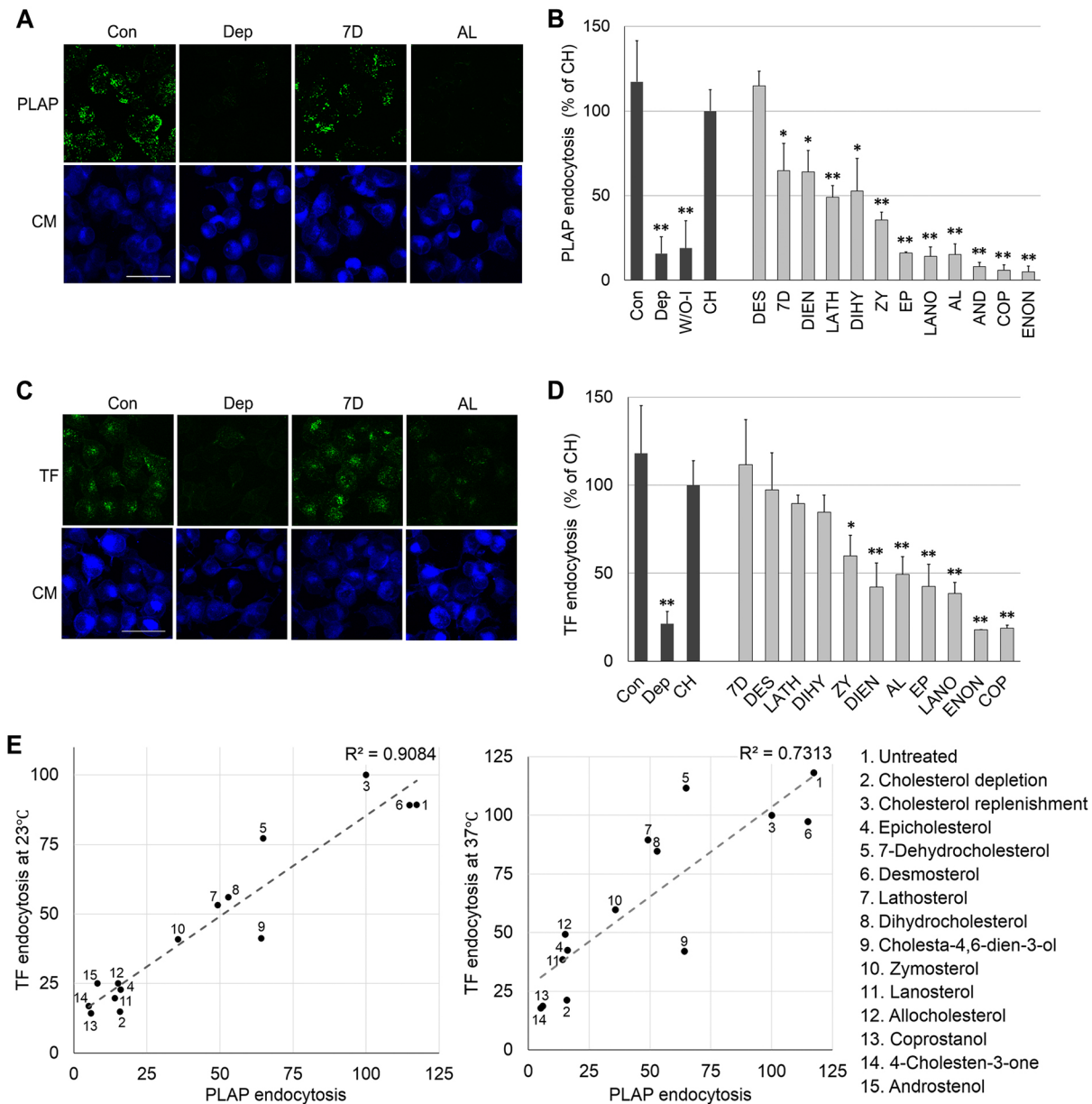


**Fig. 3. Effect of sterol substitution upon endocytosis.** (A) z-stack images of cells after cholesterol depletion and/or substitution with another sterol followed by PLAP clustering, and endocytosis and staining as in Fig. 2C. Scale bar: 50  $\mu$ m. (B) PLAP endocytosis per cell measured as in Fig. 2D. (C) z-stack images of cells after cholesterol depletion and/or substitution with another sterol followed by induction of TF endocytosis and staining as in Fig. 2E. Scale bar: 50  $\mu$ m. (D) TF endocytosis per cell measured as in Fig. 2F. In B and D, the means  $\pm$  s.d. from three experiments are shown. Values normalized to that for cholesterol replenished cells. (E) Correlation of the effects of the sterols on PLAP endocytosis (at 37°C) and TF endocytosis [at 23°C (left) or 37°C (right)]. Points are shown at mean endocytosis values. W/O-I, without internalization (incubated on ice instead of incubation at 37°C); CH, cholesterol replenished; DES, desmosterol; 7D, 7dehydrocholesterol; DIEN, cholesta-4,6-dien-3 $\beta$ -ol; LATH, lathosterol; DIHY, dihydrocholesterol; ZY, zymosterol; EP, epicholesterol; LANO, lanosterol; AL, allocholesterol; AND, 5-androsten-3 $\beta$ -ol; COP, coprostanol; ENON, 4-cholesten-3-one. Scale bars: 50  $\mu$ m. \* $P$ <0.05; \*\* $P$ <0.01 compared to 'CH' (unpaired, two-tailed Student's  $t$ -test).

of sterol removed upon a second round of exchange indicates the presence of plasma membrane/surface-accessible sterol levels that might be sufficient to support a significant amount of endocytosis (if the sterols had an ability to support endocytosis similar to that of cholesterol). Nevertheless, poor retention of sterol in surface-accessible or surface equilibrating compartments of the cells could contribute significantly to the blockage of endocytosis mediated by some sterols.

Changes in lipid packing after sterol substitution also indicated that a significant amount of substituted sterol resided in the plasma membrane. Effects of substituted sterols on lipid packing were

assayed with the plasma membrane outer leaflet probe Nile Red (NR)12S (Fig. S3B) (Kreder et al., 2015; Kucherak et al., 2010). The ratio of NR12S emission at 570 nm to that at 602 nm decreases when lipid packing decreases. Cholesterol depletion or substitution with raft-disrupting sterols (coprostanol or 4-cholesten-3-one) or with allocholesterol reduced the NR12S emission ratio relative to that in untreated cells, while the ratio recovered to the value in untreated cells upon cholesterol replenishment or substitution with desmosterol or lanosterol. Because NR12S localizes in the plasma membrane (Kreder et al., 2015; Kucherak et al., 2010), a change of the 570 nm:602 nm fluorescence ratio after sterol substitution

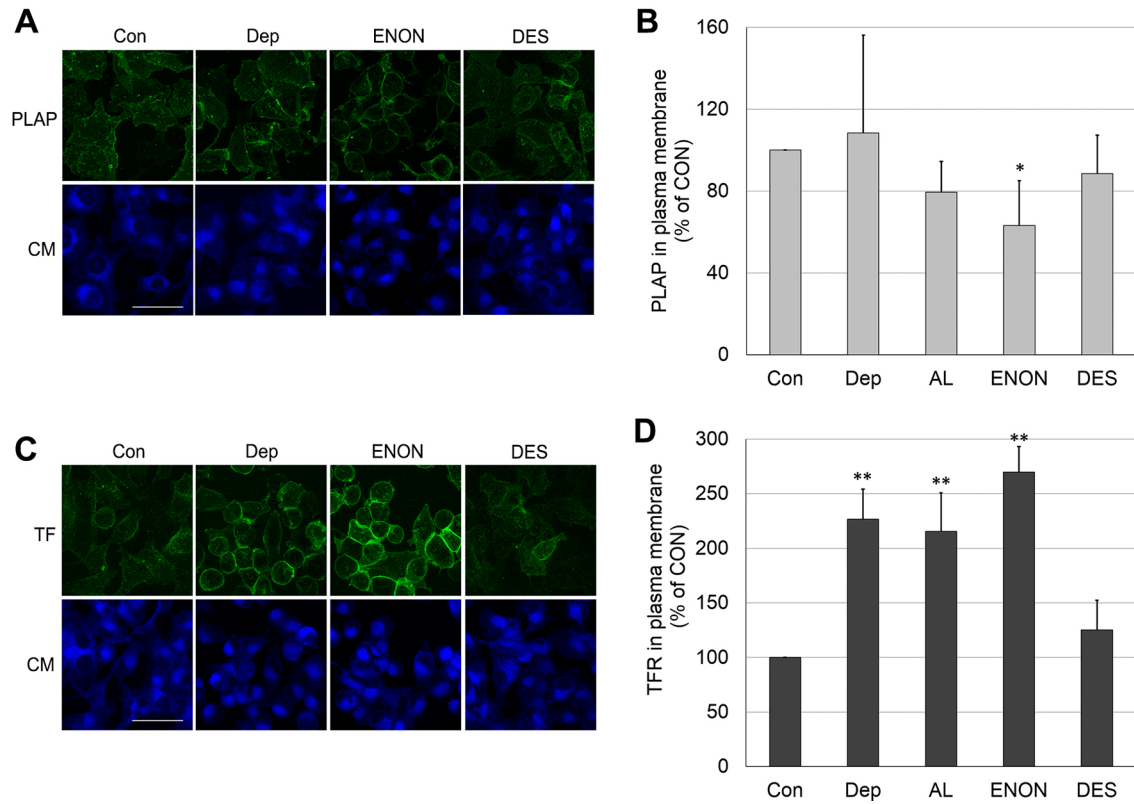


**Fig. 4. PLAP and TFR protein levels in plasma membrane after cholesterol depletion or its replacement with another sterol.** (A) Images of PLAP staining (green) on the cell plasma membrane, counter-stained with CellMask (CM, blue fluorescence). (B) Quantification of PLAP fluorescence intensity. (C) Images of TFR staining (green) on the cell plasma membrane. (D) Quantification of TFR fluorescence intensity. PLAP and TFR on the cell surface were detected by analyzing the immunofluorescence of antibody binding to cells that had been fixed after sterol manipulation. The fluorescence intensity/cell of 50 cells/experiment was then measured. Con, untreated control cells; Dep, cholesterol-depleted cells; AL, allocholesterol; ENON, 4-cholesten-3-one; DES, desmosterol. In B and D, the mean±s.d. are shown from three independent experiments. Scale bars: 50 μm. \**P*<0.05; \*\**P*<0.01 compared to 'Con' (unpaired, two-tailed Student's *t*-test).

relative to that after sterol depletion indicates the presence of sufficient substituted sterol in the outer leaflet of the plasma membrane to alter membrane physical properties. (A decrease in the

ratio could also reflect the further removal of cholesterol upon substitution, but the decrease of the 570 nm:602 nm fluorescence ratio seen with 4-cholesten-3-one is greater than that seen with

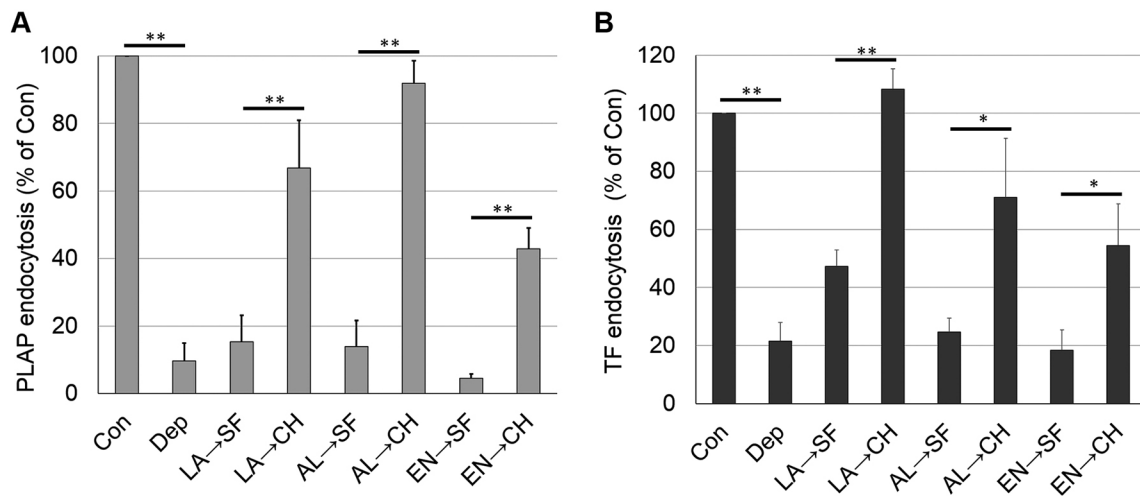


**Fig. 5. Inhibition of endocytosis by sterol substitution can be reversed by re-addition of cholesterol.** (A) Reversibility of PLAP endocytosis. (B) Reversibility of TF endocytosis. Endocytosis experiments were carried out as in substitution studies except that substitution time was shortened to 1 h and followed by a second 1 h substitution incubation with serum-free medium or cholesterol-loaded MβCD in serum-free medium. Con, untreated control cells; Dep, cholesterol-depleted cells; LA, lanosterol substituted in first incubation; AL, allocholesterol substituted in first incubation; EN, 4-cholesten-3-one substituted in first incubation; SF, serum-free medium incubated in second incubation; CH, cholesterol-substituted in second incubation. The mean±s.d. from three experiments are shown. \**P*<0.05; \*\**P*<0.01 (unpaired, two-tailed Student's *t*-test).

allocholesterol or coprostanol, see Table 1, even though substitution with the latter two sterols results in larger decreases in cholesterol levels than does substitution with 4-cholesten-3-one. Therefore, the decrease in 570 nm:602 nm fluorescence ratio with 4-cholesten-3-one likely reflects its location in the plasma membrane.) The effects of cholesterol depletion and replenishment upon lipid packing in the plasma membrane outer leaflet as measured by TMADPH anisotropy were similar to those measured with NR12S (data not shown).

Lipid packing as judged by NR12S emission is correlated to some degree with the level of endocytosis (Fig. S3C). Tight lipid packing was associated with a high level of endocytosis. However, in the case of lanosterol, endocytosis levels were low despite relatively tight lipid packing (see Discussion).

Some degree of cellular ‘rounding up’ was noted after cholesterol depletion and after substitution with some sterols. This was of concern because cellular morphology changes are often related to cytoskeletal rearrangements, which in turn might affect endocytosis (Head et al., 2014; Samaj et al., 2004). However, there was no strict connection between endocytosis and rounding up (easily measured by decreased apparent cell size, i.e. decreased cross-sectional cell area) (Fig. S4A). This conclusion was strengthened by comparing endocytosis levels to cell size for individual cells for each specific sterol substitution. Although a range of cell sizes was observed, there was no strong correlation between cell size and whether endocytosis levels were elevated or not relative to cholesterol-depleted cells (Fig. S4B).

#### Relationship between sterol properties and endocytosis – necessary and sufficient analysis

Since substituting with some sterols does not support endocytosis despite maintaining overall normal sterol levels, blockage of endocytosis involves more than large-scale membrane changes resulting from a loss of membrane mass upon removal of cholesterol. Instead, sterol must have a more direct role. From the pattern of endocytosis versus sterol structure, it is possible to define features of a sterol that are necessary and/or sufficient to support endocytosis, at least if a large enough number of sterols are studied so that a pattern can be seen.

To determine which properties of sterols were necessary and/or sufficient for efficient endocytosis, the data in Fig. 3 were sorted in terms of four properties: the ability or lack of ability to support ordered domain formation, the presence or absence of a 3 $\beta$ -OH group, the presence or absence of the cholesterol double bond between carbons 5 and 6 in the sterol B-ring, and the presence or absence of an aliphatic tail identical to that of cholesterol (see Table S1). Endocytosis levels for each sterol were then plotted for the property being considered (Fig. 6).

First, the relationship between endocytosis and the ability of a sterol to support ordered domain formation was analyzed. Sterols were divided into three categories based on previous studies in model membrane vesicles (Megha et al., 2006; Wang et al., 2004; Xu et al., 2001; Xu and London, 2000); strongly ordered domain-supporting, weakly ordered domain supporting, or ordered domain-disrupting. Based on this, the ability of a sterol to support ordered domain formation appears to be necessary, but not sufficient, for endocytosis for both clustered PLAP and TF (Fig. 6A,F). It should be noted that this pattern might reflect an effect of sterol structure on something other than their role in the formation of ordered domains in the plasma membrane (see Discussion).

The presence of a 3 $\beta$ -OH group was also found to be necessary but not sufficient for endocytosis (Fig. 6B,G). Neither 4-cholesten-

3-one, a steroid with a 3 keto group in place of a 3 OH, nor epicholesterol, a sterol that supports ordered domain formation but which has a 3 $\alpha$ -OH in place of a 3 $\beta$ -OH, could support endocytosis. Combining these observations, a sterol having both the ability to support ordered domain formation and a 3 $\beta$ -OH group was necessary and sufficient for it to support endocytosis (Fig. 6C,H).

In contrast to the properties above, the presence of a double bond between carbons 5 and 6 of the sterol B-ring was neither required nor sufficient to support endocytosis (Fig. 6D,I). Because the presence of a double bond increases the planarity of sterol rings, and because dihydrocholesterol, which lacks any double bonds, supports endocytosis, this suggests subtle changes in planarity are not critical for endocytosis. However, substitution with sterols having a carbon-5–carbon-6 double bond did result, on average, in a higher level of endocytosis than substitution with sterols that lack a carbon-5–carbon-6 double bond, which might imply local planarity does have some influence on endocytosis. In addition, coprostanol, an isomer of dihydrocholesterol that is highly bent between the A and B rings does not support endocytosis, further supporting the importance of planarity. Furthermore, having an aliphatic tail structure identical to that of cholesterol (as opposed to having extra methyl groups, a double bond in the tail or a shortened tail) was neither necessary nor sufficient for a sterol to support endocytosis (Fig. 6E,J).

#### DISCUSSION

To characterize the function of sterols in endocytosis, we used a sterol substitution method. The experiments showed a relationship between sterol structure and endocytosis that was similar for clathrin-dependent and for (at least one form of) clathrin-independent endocytosis. This suggests that some structural sterol features, membrane properties and/or a process that affects both types of endocytosis is involved. A number of sterol structural features were examined. It should be noted that, in order to demonstrate that a sterol property is not necessary to support function, it is only necessary to show that one sterol lacking the property in question is able to support function and, in order to demonstrate that a sterol property is not sufficient to support function, it is only necessary to show that one sterol having the property in question is not able to support function. However, when trying to show a property is necessary or sufficient, the more sterols studied that show a property is necessary or sufficient, the more robust the conclusion that a property is likely to be necessary or sufficient. From such an analysis, it was found that endocytosis is not likely to be absolutely dependent upon a sterol being identical to cholesterol in terms of aliphatic tail structure or double bond content. On the other hand, having a 3 $\beta$ -OH group on the sterol A-ring and the ability to promote ordered domain formation was required for a sterol to support endocytosis.

Based on these results, one possibility is that some general membrane processes dependent upon membrane domain formation are involved in endocytosis. However, it is not necessarily true that ordered domains are required for endocytosis. Because sterols that support ordered domain formation also tend to promote tight lipid packing (LaRocca et al., 2013), it could be the effect of sterol on lipid packing, rather than ordered domain formation, that is important. Lipid packing itself can alter the ability of a membrane to tolerate curvature (Kollmitzer et al., 2013), so the effect of sterol on lipid lateral packing might be more relevant than domain formation. This could involve effects of lipid packing upon membrane stiffness or cytoskeletal interactions. However, the lipid-packing measurements indicated substitution with one sterol that maintained plasma membrane outer leaflet packing (lanosterol)



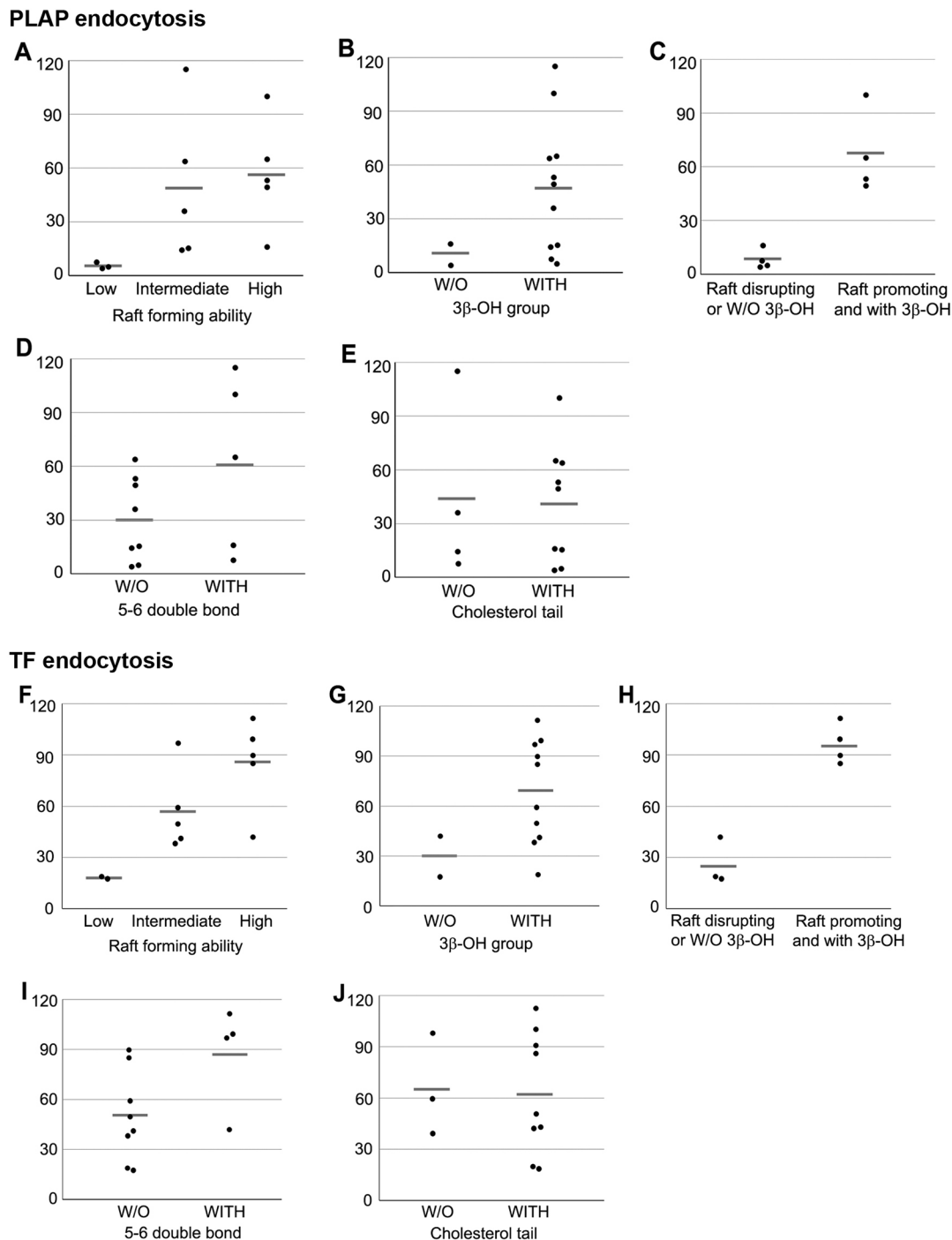


**Fig. 6. Effect of properties of sterols on PLAP and TF endocytosis.** Each dot represents each one of the sterols in the categories shown and horizontal gray bars are average (mean) level of the endocytosis in each category. (A–E) Relationships between sterol properties (x-axis) and PLAP endocytosis level (y-axis, percentage of cholesterol replenished). (F–J) Relationships between sterol properties (x-axis) and TF endocytosis level (y-axis, percentage of cholesterol replenished). (A) Relationship between raft-forming ability (high, intermediate and low) and PLAP endocytosis. (B) Effect of the presence (WITH) or absence (W/O) of the 3 $\beta$ -OH group on PLAP endocytosis. (C) Effect of having both raft-promoting ability and the 3 $\beta$ -OH group upon the PLAP endocytosis. (D) Effect of the double bond between carbons 5 and 6 in the B-ring upon PLAP endocytosis. (E) Relationship between cholesterol tail structure and PLAP endocytosis. (F) Relationship between raft-forming ability and TF endocytosis. (G) Effect of the presence or absence of the 3 $\beta$ -OH group and TF endocytosis. (H) Effect of having both raft-promoting ability and the 3 $\beta$ -OH group upon TF endocytosis. (I) Effect of the double bond between carbons 5 and 6 in the B-ring upon TF endocytosis. (J) Relationship between cholesterol tail structure and TF endocytosis.

and did not support endocytosis, whereas a sterol that reduced this packing (allocholesterol) supported some degree of endocytosis for TF at 37°C. In addition, previous studies have shown membrane domain formation can be involved in sorting of both lipids and proteins (Dupree et al., 1993; Mayor et al., 1993; Sorre et al., 2009;

Wang et al., 2000). Nevertheless, these two explanations for what sterol properties are crucial for endocytosis are not mutually exclusive. Furthermore, it is unlikely that direct interaction of the endocytosed proteins with Lo domains is involved, because although GPI-anchored proteins have some affinity for ordered

domains, especially when clustered (Ge et al., 2014; Kahya et al., 2005; Schroeder et al., 1998), the TFR is a classical marker for Ld domains (Garcia-Marcos et al., 2006; Gaus et al., 2003, 2005; Macdonald and Pike, 2005; Pike et al., 2005).

Even if Lo domains are involved, it does not mean that such domains are present in the plasma membrane. The observation that some sterols substituted into the plasma membrane can partly reside in internal compartments is consistent with sterol substitution affecting the physical state or domain formation in internal membranes, and also consistent with the role of internal membrane domains in membrane recycling, as proposed in several studies (Mukherjee et al., 1999; Refa'ei et al., 2011; Roux et al., 2005). This means a possible explanation for the inhibition of endocytosis is that a domain-dependent block in a step in membrane recycling shuts down endocytosis because membrane endocytosis needs to be balanced by membrane recycling to maintain plasma membrane lipid and protein levels. However, this seems unlikely in view of the observation that blocked endocytosis resulting from cholesterol depletion led to increased levels of TFR in the plasma membrane. Furthermore, cholesterol depletion increases the rate of recycling of GPI-anchored proteins (Mayor et al., 1998). This suggests that cholesterol depletion causes a block in endocytosis itself, and that recycling of TFR from internal compartments to the plasma membrane continues after internalization of TFR into endocytic vesicles is blocked.

Altering sterols may also sometimes act by directly altering the activity of specific proteins. It has been reported from molecular dynamics studies, that specific sterols can have different specific interactions with membrane proteins that alter their ability to undergo conformational changes (Manna et al., 2016). For example, the alteration of the 3 $\beta$ -OH group of cholesterol to the 3 $\alpha$ -OH group on epicholesterol decreases the planarity of the sterol, and might change its ability to fit into the binding site on a protein (Hulce et al., 2013). There are several examples in which altering sterol changes protein–sterol interaction. Oxytocin receptor, a G-protein-coupled receptor, needs to interact with cholesterol through specific structures to have normal level of ligand binding, and the 3 $\beta$ -OH group is one of the features critical for the ligand binding (Gimpl et al., 1997). The function of serotonin receptor 1A (also known as HTR1A), another G-protein-coupled receptor, was also lost by changing the orientation of the sterol OH group from 3 $\beta$  to 3 $\alpha$  (Jafurulla et al., 2014). In a study of inward-rectifier K<sup>+</sup> channels it was shown that cholesterol depletion and replacement of cholesterol with epicholesterol had the same effect upon current density (Romanenko et al., 2002). Interactions between intermediate-conductance (IK1, also known as KCNN4) and large-conductance (maxi-K) Ca<sup>2+</sup>-activated K<sup>+</sup> channels (also known as KCNMA1) was also sensitive to the orientation of the sterol 3-OH group (Romanenko et al., 2009). Finally, it was found in another study that perfringolysin O binds to sterols having a 3 $\beta$ -OH group but not to epicholesterol in lipid model membrane vesicles (Lin and London, 2013). Consistent with the hypothesis that the effect of a 3 $\alpha$ -OH does not involve its physical properties, epicholesterol is able to support Lo domain formation in model membrane vesicles (Beattie et al., 2005; Xu and London, 2000).

## MATERIALS AND METHODS

### Cells

MDA-MB-231 breast cancer cells were from the ATCC. Cells stably expressing PLAP (Berger et al., 1987) were generated by subcloning the PLAP cDNA from pBC12 into pcDNA3, transfecting MDA-MB-231 cells by using Lipofectamine 2000 (ThermoFisher Scientific, Waltham, MA) in conditions recommended by the supplier, and selection of a cloned

drug-resistant cell line using G418 (Sigma-Aldrich, St Louis, MO). Cells were maintained in Dulbecco's modified Eagle medium (DMEM) (Gibco, Grand Island, NY) supplemented with iron-fortified 10% bovine calf serum (SAFC Biosciences, Lenexa, KS) or 10% iron-supplemented calf serum (Atlanta Biologicals, Flowery Branch, GA), 100 U/ml penicillin and 100  $\mu$ g/ml streptomycin (Gibco), and 600  $\mu$ g/ml G418 at 37°C and 5% CO<sub>2</sub>.

### Materials

Dulbecco's phosphate-buffered saline (DPBS, containing 200 mg/l potassium chloride, 200 mg/l potassium phosphate monobasic, 8 g/l sodium chloride and 2.16 g/l sodium phosphate dibasic) for tissue-culture, Hank's balanced salt solution (HBSS, containing 140 mg/l calcium chloride, 100 mg/l magnesium chloride, 100 mg/l magnesium sulfate, 400 mg/l potassium chloride, 60 mg/l potassium phosphate monobasic, 350 mg/l sodium bicarbonate, 8000 mg/l sodium chloride, 48 mg/l sodium phosphate dibasic anhydrous, and 1000 mg/l D-glucose) and trypsin-EDTA were obtained from Gibco. Bradford protein assay reagent and 10 $\times$  phosphate-buffered saline (PBS; 10 mM sodium phosphate, 150 mM NaCl, pH 7.4), used for immunofluorescence and the TF endocytosis assay, were purchased from Bio-Rad Laboratories (Hercules, CA). BSA was obtained from Millipore (Kankakee, IL). Cholesterol, desmosterol and zymosterol were purchased from Avanti Polar Lipids (Alabaster, AL). Dihydrocholesterol, 7-dehydrocholesterol (Fluka brand), lanosterol, M $\beta$ CD, 1,6-diphenyl-1,3,5-hexatriene (DPH), BSTFA-TMCS [N,O-bis(trimethylsilyl)-trifluoroacetamide-trimethylchlorosilane] reagent and paraformaldehyde (PFA) were purchased from Sigma-Aldrich. Epicholesterol (5-cholesten-3 $\alpha$ -ol), allocholesterol (4-cholesten-3 $\beta$ -ol), coprostanol, androstenol (5-androsten-3 $\beta$ -ol), 4-cholesten-3-one (cholestenone) and cholesta-4,6-dien-3 $\beta$ -ol were obtained from Steraloids (Newport, RI). Lathosterol was purchased from Research Plus (Manasquan, NJ). Sterols generally appeared as single bands on thin-layer chromatography, but lanosterol was purchased as a mixture with ~65% lanosterol, the remainder likely being dihydrolanosterol. We did not detect sterol impurities on TLC, except for lanosterol, which is probably due to the presence of 30% dihydrolanosterol. Mouse monoclonal anti-alkaline phosphatase (ALPP) antibody (8B6) was purchased from Novus Biologicals (NB110-3638, Littleton, CO), diluted two-fold with glycerol before storage and diluted 1:25 before use. Mouse monoclonal anti-TFR antibody (MEM-189) was purchased from Abcam (ab1086, Cambridge, MA), diluted two-fold with glycerol before storage and diluted 1:250 before use. 1-(4-trimethylammoniumphenyl)-6-phenyl-1,3,5-hexatriene p-toluenesulfonate (TMADPH) and Alexa Fluor 488 (AF488)-goat anti-mouse-IgG antibody (A11001), AF488-TF and CellMask™ Deep Red Plasma membrane stain were a Molecular Probes brand, purchased from Life Technologies (Eugene, OR). The AF488-goat anti-mouse-IgG antibody (A11001) was diluted two fold with glycerol before storage and then diluted 1:25 before use in PLAP endocytosis experiments, or 1:250 for determination of surface PLAP or TFR. High-performance thin-layer chromatography (HP-TLC) plates (Silica Gel 60) were purchased from VWR International (Batavia, IL). Hexanes, isopropanol, citric acid and sodium chloride were purchased from Fisher Scientific (Fair Lawn, NJ). VECTASHIELD® mounting medium was purchased from Vector Laboratories (Burlingame, CA).

### Preparation of M $\beta$ CD loaded with sterol

M $\beta$ CD dissolved in water, and sterols dissolved in chloroform were mixed in glass tubes to prepare samples with the desired concentrations. The mixtures were dried under N<sub>2</sub> gas for 10–20 min, and then dried by high vacuum for 1–2 h. Next, 1 ml of serum-free DMEM was added to each tube, and the solutions were sonicated with an ultrasonic cleaner (model 8845-3, Cole-Parmer Instrument Company, Chicago, IL) for ~2 min. Solutions were incubated overnight at 37°C in a shaking incubator. When necessary, serum-free DMEM was then added in the tubes to make up to the final volume (which diluted them up to five-fold), and the solutions filtered through a syringe filter (0.22  $\mu$ m, Sarstedt, Nümbrecht, Germany) to remove undissolved sterol. Unless otherwise noted, the final solutions, assuming undissolved sterol was negligible, contained 0.1 mM cholesterol mixed with 2.5 mM M $\beta$ CD, or for all other sterols 0.4 mM sterol with 2.5 mM M $\beta$ CD.

### Cholesterol depletion and sterol substitution in cells

Cells were prepared 1 day prior to sterol substitution. For PLAP and TF endocytosis assays,  $6 \times 10^5$  cells were plated on a coverslip placed in a 35 mm dish. It should be noticed that cells grown on coverslips and placed in 35 mm wells, spread and adhered slightly less well than cells that were grown directly on the wells. To purify lipids from cells for analysis,  $1.2 \times 10^6$  cells were plated on a 60 mm dish. The next day, the cells were washed twice with 2 ml (35 mm) to 3 ml (60 mm) DPBS, then cellular cholesterol was depleted by incubation with 10 mM M $\beta$ CD in serum-free DMEM for 30 min in a 37°C incubator. For sterol substitution, the cells were then washed once with 2 ml (35 mm) to 3 ml (60 mm) DPBS, and the solution containing M $\beta$ CD loaded with sterol (1 ml for 35 mm wells, 1.5 ml for 60 mm plates) was added to the cells, followed by incubation for 2 h at 37°C. The lower ratio of cyclodextrin-containing solution added to the surface area in the 60 mm dishes may slightly underestimate depletion and exchange in the 35 mm wells. For analyzing the reversibility of the effects of sterol substitution, two steps of substitution (first step, substitution with endocytosis-inhibiting sterol; second step, replenishing with cholesterol or treatment with serum-free DMEM) were carried out with 1 h for each substitution step instead of a single 2 h incubation to avoid potential side effects caused by prolonged exposure time to M $\beta$ CD.

### PLAP endocytosis assay

After cholesterol depletion or sterol substitution, the plates containing the cells were placed on ice and washed twice with 2 ml cold 1× PBS (i.e. placed on ice). Mouse monoclonal anti-PLAP IgG was prepared at 20  $\mu$ g/ml in HBSS containing 3% w/v BSA. Each plate was incubated with 100  $\mu$ l of anti-PLAP antibody solution at 4°C for 15 min, then placed on ice, and washed twice with 2 ml cold 1× PBS. Next, 100  $\mu$ l of AF488-conjugated goat anti-mouse-IgG antibody [prepared at 40  $\mu$ g/ml in HBSS with 3% (w/v) BSA] was added to the cells and incubated for 15 min at 4°C. Then the plates were again washed twice with 2 ml cold 1× PBS. Pre-warmed 3% (w/v) BSA in HBSS was then added, and plates were incubated at 37°C for 20 min to induce internalization of PLAP. Cells were placed on ice to stop internalization and washed twice with 2 ml cold 1× PBS. By addition of cold PBS to the cells and incubating them on ice instead of 37°C, we also prepared an untreated control in which internalization was not induced because the cells were kept on ice. Cells were moved into a cool room (16–18°C) and acid-washed three times (incubating in acid for 3 min each time) with 2 ml of 100 mM citric acid and 140 mM NaCl, adjusted to pH 1.75 with HCl. Fig. S5 shows the acid washing worked properly, with over 90% of fluorescence on the cell surface removed. Then cells were washed twice with 2 ml cold 1× PBS and, after removal of the washing solution, fixed with 2 ml of 3% (w/v) PFA in PBS for 10 min on ice followed by 20 min at room temperature. After fixation, cells were washed three times with 2 ml 1× PBS at room temperature. Cellular plasma membrane staining was performed with 100  $\mu$ l CellMask solution diluted to 4  $\mu$ l/ml in HBSS with 3% (w/v) BSA for 2–5 min at room temperature. After washing with 2 ml 1× PBS at room temperature, coverslips were taken from the dishes and mounted on slides using VECTASHIELD® mounting medium.

The minimal fluorescence present after acid washing when cells are not exposed to temperatures over 18°C, could be due to the residual baseline endocytosis plus a small amount of autofluorescence. To correct for this, we only consider the increase over the background value of fluorescence (that in these low temperature samples) as representing sterol-supported endocytosis.

### Transferrin endocytosis assay

After cholesterol depletion or sterol substitution, cells were washed with 2 ml DPBS at room temperature three times. Then 100  $\mu$ l of 50  $\mu$ g/ml AF488–TF in serum-free DMEM was added to the cells, which were incubated at 37°C for 7 min (or at 23°C for 10 min) to allow endocytosis to occur. Cells were then placed on ice and washed three times with 2 ml cold 1× PBS. Acid washing was performed on ice with the solution described above and carried out three times with a 3 min incubation each time. Cells were then washed three times with 2 ml cold 1× PBS. Cell fixation, CellMask staining and mounting were performed as described above.

### Immunostaining of PLAP and TFR on cellular plasma membrane

Cells were prepared the same as for endocytosis experiments. After cholesterol depletion or sterol substitution, cells were washed with 2 ml DPBS three times and then fixed as above. Fixed cells were washed with 1× PBS three times and surface PLAP and TFR levels were measured by measuring immunofluorescence as follows: cells were incubated with blocking solution [3% (w/v) BSA in HBSS] for 30 min at room temperature, then 100  $\mu$ l of primary antibody solution [20  $\mu$ g/ml mouse monoclonal anti-PLAP IgG or 2  $\mu$ g/ml mouse monoclonal anti-TFR IgG in HBSS containing 3% (w/v) BSA] was added to cells and incubated for 1 h at room temperature. Cells were washed with 1× PBS three times and incubated with 100  $\mu$ l of AF488-conjugated goat anti-mouse-IgG antibody (prepared at 2  $\mu$ g/ml in HBSS with 3% w/v BSA) at room temperature for 1 h. Then cells were washed with 1× PBS three times and CellMask staining and mounting were performed as above.

### Image analysis of stained cells

Fluorescently stained cells were examined by confocal microscopy, and *z*-stack images were taken using a Zeiss 510 Meta NLO confocal microscope. From the images, the levels of PLAP and TF endocytosis were analyzed by using the ImageJ 1.50C program kindly supplied by Wayne Rasband of National Institutes of Health. For PLAP endocytosis analysis, 3–7 images of each of three samples prepared independently on different days were taken at 630× magnification (analyzing  $\geq 50$  cells per sample). The number of internalized PLAP puncta and cell numbers were counted by using the ImageJ program and the puncta/cell calculated. In case of TF endocytosis, two to four images of each of three samples prepared independently on different days were taken at 600× magnification and analyzed by using the ImageJ program. The area of a cell (visualized by blue CellMask fluorescence) was determined, and the integrated density of green fluorescence (from AF488–TF) within the cell area was measured (integrated density = mean intensity of green fluorescence  $\times$  cell area). For each sample, the background green fluorescence intensity was also measured in five spots outside of cells and averaged. Then, corrected total cell fluorescence (CTCF) was calculated using the equation: CTCF = integrated density – (area of selected cell  $\times$  mean background fluorescence per unit area). For each sample, CTCF was calculated for a total of 50 cells.

### Isolation of lipids and proteins from cells

After cholesterol depletion or sterol substitution, cells were washed three times with 3 ml DPBS at room temperature and, after removal of the last washing solution, 1 ml of mixed hexanes and isopropanol (2:1, v/v) was added to each well (60 mm dish). After incubation at room temperature for 30 min while shaking gently on a rocker, the solution was harvested in a glass tube and dried under N<sub>2</sub> gas. Then it was stored at –20°C. The residue in the tissue culture dish after extraction of lipid was used for protein isolation. To do this, the dishes were dried in air, and then 1 ml of 1 M NaOH was added. After incubation at room temperature for 1 h while shaking gently on a rocker, the solution was harvested in a 1.5 ml plastic tube and stored at –20°C (Davis, 2011; Eberhart et al., 1998; Hara and Radin, 1978).

### HP-TLC

In the glass tube containing dried lipids from cells, 300  $\mu$ l of methanol-chloroform (1:1, v/v) was added and then the tube was vortexed. A 30  $\mu$ l aliquot was removed and loaded on a HP-TLC plate alongside various amounts of sterol standards. After drying, the plate was placed in a tank containing mixed hexanes and ethyl acetate (3:2, v/v) and the sample was then chromatographed until the solvent reached the top of the TLC plate. Then the plate was removed, air dried and sprayed with a solution of 3% (w/v) cupric acetate and 8% phosphoric acid (v/v) dissolved in water. The plate was redried and heated at 200°C in an oven until the charred lipid bands were clearly detectable. The TLC plate was scanned and intensity in each lipid band was measured with the ImageJ program and quantified by comparison to a standard curve of intensity versus amount derived from the intensity in the standards loaded onto the plate using the SlideWrite Plus program (Advanced Graphics Software, Rancho Santa Fe, CA). Sterol amount was then normalized to protein level in the dish from which the lipids were purified.

### Protein quantification

Protein levels from cells were quantified by using the Bradford method (Bradford, 1976). The cellular protein-containing solution obtained as above was diluted with water and the Bradford solution reagent mixed in the ratio 31:8:1 or 79:20:1 (v/v; water:Bradford solution:protein extract). The standards were 1.5–25 µg/ml of BSA. Samples were incubated at room temperature for 20 min, and then absorbance at 595 nm was measured using a spectrophotometer. Protein concentration from cells was then calculated from comparison to the absorbance versus concentration curve constructed from the BSA standards.

### Quantification of sterol species by GC-MS

Sterol derivatization, detection and analysis was performed by GC-MS using the methods described previously (Chang et al., 2014; Nes et al., 2009; Singh et al., 2013) using an Agilent 7890 GC-MS machine (Agilent Technologies, Santa Clara, CA). Briefly, extracted and base-hydrolyzed lipid samples were derivatized using 100 µl BSTFA-TMCS reagent at 85°C for 90 min. Next, 50 µl n-hexane was added to the derivatized sample and vortexed. The samples were then analyzed by using a 30 m (0.25 µm) DB5-MS column on an Agilent 7890 GC-MS. The initial column temperature of 10°C was held for 0.5 min and ramped at 35°C/min to 240°C, then at 3°C/min to 260°C and then at 1.5°C/min to 305°C with a hold of 2 min. All EI-mass spectra were recorded at 70 eV with ion source temperature of 230°C. The front inlet temperature was kept at 290°C and the MSD transfer line temperature was kept at 280°C. The retention time and mass spectral patterns of the appropriate sterol standards were used as a reference. Ergosterol (25 µg), a non-mammalian sterol, was added as an internal standard for these analyses prior to lipid extraction. Sterol species content in each sample were quantified based on standard calibration curves and normalized to the lipid dry mass in milligrams. All experiments were performed in triplicates.

### NR12S fluorescence measurements

Cells ( $6 \times 10^5$ ) were plated on a 35 mm dish. The next day, cholesterol depletion and replenishment or sterol substitution were performed as described above. Cells were washed once with 2 ml pre-warmed HBSS and treated with 0.7 ml trypsin-EDTA for 3 min at 37°C. After 3 ml HBSS was added into the dish, the now-detached cells were harvested and transferred into a 15 ml tube. After centrifugation (Eppendorf Centrifuge 5810) for 3 min at 1000 rpm (200 g), the supernatant solution was discarded and cell pellets washed with 3 ml HBSS before being recentrifuged for 3 min at 1000 rpm. The final cell pellet was resuspended in 2 ml HBSS containing 40 nM NR12S (from an 80 µM stock solution dissolved in DMSO) and incubated for 7 min in the dark at room temperature. Fluorescence emission intensity was measured at both 570 nm and 602 nm (with excitation at 520 nm) at room temperature or 37°C and the ratio of emission intensity at 570 nm /intensity at 602 nm was calculated to determine cell plasma membrane order.

### Acknowledgements

The authors thank Dr Andrey Klymchenko (University of Strasbourg, Strasbourg, France) for the gift of NR12S, and Anne Ostermeyer-Fay (Stony Brook University, Stony Brook, NY) for making the PLAP-transfected MDA-MB-231 cell line.

### Competing interests

The authors declare no competing or financial interests.

### Author contributions

Conceptualization: J.K., A.S., M.D., D.B., E.L.; Formal analysis: J.K., A.S., M.D., D.B., E.L.; Investigation: J.K., A.S., M.D., D.B., E.L.; Resources: D.B.; Writing - original draft: J.K., E.L.; Writing - review & editing: J.K., D.B., E.L.; Supervision: D.B., E.L.; Funding acquisition: M.D., E.L.

### Funding

This work was supported by the National Institutes of Health [GM 099892 and GM 122493 to E.L., and AI125770 to M.D.P.]. Deposited in PMC for release after 12 months.

### Supplementary information

Supplementary information available online at <http://jcs.biologists.org/lookup/doi/10.1242/jcs.201731.supplemental>

### References

- Bang, B., Gniadecki, R. and Gajkowska, B. (2005). Disruption of lipid rafts causes apoptotic cell death in HaCaT keratinocytes. *Exp. Dermatol.* **14**, 266–272.
- Baumgart, T., Hammond, A. T., Sengupta, P., Hess, S. T., Holowka, D. A., Baird, B. A. and Webb, W. W. (2007). Large-scale fluid/fluid phase separation of proteins and lipids in giant plasma membrane vesicles. *Proc. Natl. Acad. Sci. USA* **104**, 3165–3170.
- Beattie, M. E., Veatch, S. L., Stottrup, B. L. and Keller, S. L. (2005). Sterol structure determines miscibility versus melting transitions in lipid vesicles. *Biophys. J.* **89**, 1760–1768.
- Berger, J., Howard, A. D., Gerber, L., Cullen, B. R. and Udenfriend, S. (1987). Expression of active, membrane-bound human placental alkaline phosphatase by transfected simian cells. *Proc. Natl. Acad. Sci. USA* **84**, 4885–4889.
- Bradford, M. M. (1976). A rapid and sensitive method for the quantitation of microgram quantities of protein utilizing the principle of protein-dye binding. *Anal. Biochem.* **72**, 248–254.
- Brown, D. A. (2006). Lipid rafts, detergent-resistant membranes, and raft targeting signals. *Physiology (Bethesda)* **21**, 430–439.
- Brown, D. A. and London, E. (1997). Structure of detergent-resistant membrane domains: does phase separation occur in biological membranes? *Biochem. Biophys. Res. Commun.* **240**, 1–7.
- Brown, A. J., Sun, L., Feramisco, J. D., Brown, M. S. and Goldstein, J. L. (2002). Cholesterol addition to ER membranes alters conformation of SCAP, the SREBP escort protein that regulates cholesterol metabolism. *Mol. Cell* **10**, 237–245.
- Campbell, S., Gaus, K., Bittman, R., Jessup, W., Crowe, S. and Mak, J. (2004). The raft-promoting property of virion-associated cholesterol, but not the presence of virion-associated Brij 98 rafts, is a determinant of human immunodeficiency virus type 1 infectivity. *J. Virol.* **78**, 10556–10565.
- Cerneus, D. P., Ueffing, E., Posthuma, G., Strous, G. J. and van der Ende, A. (1993). Detergent insolubility of alkaline phosphatase during biosynthetic transport and endocytosis. Role of cholesterol. *J. Biol. Chem.* **268**, 3150–3155.
- Chadda, R., Howes, M. T., Plowman, S. J., Hancock, J. F., Parton, R. G. and Mayor, S. (2007). Cholesterol-sensitive Cdc42 activation regulates actin polymerization for endocytosis via the GEEC pathway. *Traffic* **8**, 702–717.
- Chang, Y. C., Lamichhane, A. K., Garraffo, H. M., Walter, P. J., Leerkes, M. and Kwon-Chung, K. J. (2014). Molecular mechanisms of hypoxic responses via unique roles of Ras1, Cdc24 and Ptp3 in a human fungal pathogen *Cryptococcus neoformans*. *PLoS Genet.* **10**, e1004292.
- Cheng, H.-T., Megha, and London, E. (2009). Preparation and properties of asymmetric vesicles that mimic cell membranes: effect upon lipid raft formation and transmembrane helix orientation. *J. Biol. Chem.* **284**, 6079–6092.
- Davis, W. Jr. (2011). The ATP-binding cassette transporter-2 (ABCA2) regulates cholesterol homeostasis and low-density lipoprotein receptor metabolism in N2a neuroblastoma cells. *Biochim. Biophys. Acta* **1811**, 1152–1164.
- Diaz-Rohrer, B., Levental, K. R. and Levental, I. (2014). Rafting through traffic: Membrane domains in cellular logistics. *Biochim. Biophys. Acta* **1838**, 3003–3013.
- Doherty, G. J. and McMahon, H. T. (2009). Mechanisms of endocytosis. *Annu. Rev. Biochem.* **78**, 857–902.
- Dupree, P., Parton, R. G., Raposo, G., Kurzchalia, T. V. and Simons, K. (1993). Caveolae and sorting in the trans-Golgi network of epithelial cells. *EMBO J.* **12**, 1597–1605.
- Eberhart, G. P., Mendez, A. J. and Freeman, M. W. (1998). Decreased cholesterol efflux from fibroblasts of a patient without Tangier disease, but with markedly reduced high density lipoprotein cholesterol levels. *J. Clin. Endocrinol. Metab.* **83**, 836–846.
- Fahrenholz, F., Klein, U. and Gimpl, G. (1995). Conversion of the myometrial oxytocin receptor from low to high affinity state by cholesterol. *Adv. Exp. Med. Biol.* **395**, 311–319.
- Garcia-Marcos, M., Pochet, S., Tandel, S., Fontanils, U., Astigarraga, E., Fernández-González, J. A., Kumps, A., Marino, A. and Dehay, J. P. (2006). Characterization and comparison of raft-like membranes isolated by two different methods from rat submandibular gland cells. *Biochim. Biophys. Acta* **1758**, 796–806.
- Gaus, K., Gratton, E., Kable, E. P., Jones, A. S., Gelissen, I., Kritharides, L. and Jessup, W. (2003). Visualizing lipid structure and raft domains in living cells with two-photon microscopy. *Proc. Natl. Acad. Sci. USA* **100**, 15554–15559.
- Gaus, K., Rodriguez, M., Ruberu, K. R., Gelissen, I., Sloane, T. M., Kritharides, L. and Jessup, W. (2005). Domain-specific lipid distribution in macrophage plasma membranes. *J. Lipid Res.* **46**, 1526–1538.
- Gaus, K., Le Lay, S., Balasubramanian, N. and Schwartz, M. A. (2006). Integrin-mediated adhesion regulates membrane order. *J. Cell Biol.* **174**, 725–734.
- Ge, Y., Siegel, A. P., Jordan, R. and Naumann, C. A. (2014). Ligand binding alters dimerization and sequestering of urokinase receptors in raft-mimicking lipid mixtures. *Biophys. J.* **107**, 2101–2111.

- George, K. S., Elyassaki, W., Wu, Q. and Wu, S. (2012). The role of cholesterol in UV light B-induced apoptosis. *Photochem. Photobiol.* **88**, 1191–1197.
- Gimpl, G., Burger, K. and Fahrenholz, F. (1997). Cholesterol as modulator of receptor function. *Biochemistry* **36**, 10959–10974.
- Gniadecki, R. (2004). Depletion of membrane cholesterol causes ligand-independent activation of Fas and apoptosis. *Biochem. Biophys. Res. Commun.* **320**, 165–169.
- Hamilton, T. A. (1983). Receptor-mediated endocytosis and exocytosis of transferrin in Concanavalin A-stimulated rat lymphoblasts. *J. Cell. Physiol.* **114**, 222–228.
- Hara, A. and Radin, N. S. (1978). Lipid extraction of tissues with a low-toxicity solvent. *Anal. Biochem.* **90**, 420–426.
- Head, B. P., Patel, H. H. and Insel, P. A. (2014). Interaction of membrane/lipid rafts with the cytoskeleton: impact on signaling and function: membrane/lipid rafts, mediators of cytoskeletal arrangement and cell signaling. *Biochim. Biophys. Acta* **1838**, 532–545.
- Holz, R. W. (1974). The effects of the polyene antibiotics nystatin and amphotericin B on thin lipid membranes. *Ann. N. Y. Acad. Sci.* **235**, 469–479.
- Huang, Z. and London, E. (2013). Effect of cyclodextrin and membrane lipid structure upon cyclodextrin-lipid interaction. *Langmuir* **29**, 14631–14638.
- Hulce, J. J., Cognetta, A. B., Niphakis, M. J., Tully, S. E. and Cravatt, B. F. (2013). Proteome-wide mapping of cholesterol-interacting proteins in mammalian cells. *Nat. Methods* **10**, 259–264.
- Jafurulla, M., Rao, B. D., Sreedevi, S., Ruyschaert, J.-M., Covey, D. F. and Chattopadhyay, A. (2014). Stereospecific requirement of cholesterol in the function of the serotonin1A receptor. *Biochim. Biophys. Acta* **1838**, 158–163.
- Kahya, N., Brown, D. A. and Schwille, P. (2005). Raft partitioning and dynamic behavior of human placental alkaline phosphatase in giant unilamellar vesicles. *Biochemistry* **44**, 7479–7489.
- Kalyana Sundaram, R. V., Li, H., Bailey, L., Rashad, A. A., Aneja, R., Weiss, K., Huynh, J., Bastian, A. R., Papazoglou, E., Abrams, C. et al. (2016). Impact of HIV-1 membrane cholesterol on cell-independent lytic inactivation and cellular infectivity. *Biochemistry* **55**, 447–458.
- Kim, J. H. and London, E. (2015). Using sterol substitution to probe the role of membrane domains in membrane functions. *Lipids* **50**, 721–734.
- Kinoshita, M., Suzuki, K. G. N., Matsumori, N., Takada, M., Ano, H., Morigaki, K., Abe, M., Makino, A., Kobayashi, T., Hirose, K. M. et al. (2017). Raft-based sphingomyelin interactions revealed by new fluorescent sphingomyelin analogs. *J. Cell Biol.* **216**, 1183–1204.
- Kirkham, M., Fujita, A., Chadda, R., Nixon, S. J., Kurzchalia, T. V., Sharma, D. K., Pagano, R. E., Hancock, J. F., Mayor, S. and Parton, R. G. (2005). Ultrastructural identification of uncoated caveolin-independent early endocytic vesicles. *J. Cell Biol.* **168**, 465–476.
- Klein, U., Gimpl, G. and Fahrenholz, F. (1995). Alteration of the myometrial plasma membrane cholesterol content with beta-cyclodextrin modulates the binding affinity of the oxytocin receptor. *Biochemistry* **34**, 13784–13793.
- Kollmitzer, B., Heftberger, P., Rappolt, M. and Pabst, G. (2013). Monolayer spontaneous curvature of raft-forming membrane lipids. *Soft Mat.* **9**, 10877–10884.
- Komura, N., Suzuki, K. G. N., Ando, H., Konishi, M., Koikeda, M., Imamura, A., Chadda, R., Fujiwara, T. K., Tsuboi, H., Sheng, R. et al. (2016). Raft-based interactions of gangliosides with a GPI-anchored receptor. *Nat. Chem. Biol.* **12**, 402–410.
- Kreder, R., Pyrshev, K. A., Darwich, Z., Kucherak, O. A., Mely, Y. and Klymchenko, A. S. (2015). Solvatochromic Nile Red probes with FRET quencher reveal lipid order heterogeneity in living and apoptotic cells. *ACS Chem. Biol.* **10**, 1435–1442.
- Kristoffersen, E. K. (2000). Placental Fc receptors and the transfer of maternal IgG. *Transfus. Med. Rev.* **14**, 234–243.
- Kucherak, O. A., Oncul, S., Darwich, Z., Yushchenko, D. A., Arntz, Y., Didier, P., Mély, Y. and Klymchenko, A. S. (2010). Switchable Nile Red-based probe for cholesterol and lipid order at the outer leaflet of biomembranes. *J. Am. Chem. Soc.* **132**, 4907–4916.
- LaRocca, T. J., Crowley, J. T., Cusack, B. J., Pathak, P., Benach, J., London, E., Garcia-Monco, J. C. and Benach, J. L. (2010). Cholesterol lipids of *Borrelia burgdorferi* form lipid rafts and are required for the bactericidal activity of a complement-independent antibody. *Cell Host Microbe* **8**, 331–342.
- LaRocca, T. J., Pathak, P., Chiantia, S., Toledo, A., Silvius, J. R., Benach, J. L. and London, E. (2013). Proving lipid rafts exist: membrane domains in the prokaryote *Borrelia burgdorferi* have the same properties as eukaryotic lipid rafts. *PLoS Pathog.* **9**, e1003353.
- Le, P. U., Guay, G., Altschuler, Y. and Nabi, I. R. (2002). Caveolin-1 is a negative regulator of caveolae-mediated endocytosis to the endoplasmic reticulum. *J. Biol. Chem.* **277**, 3371–3379.
- Lin, Q. and London, E. (2013). Transmembrane protein (perfringolysin o) association with ordered membrane domains (rafts) depends upon the raft-associating properties of protein-bound sterol. *Biophys. J.* **105**, 2733–2742.
- London, E. (2005). How principles of domain formation in model membranes may explain ambiguities concerning lipid raft formation in cells. *Biochim. Biophys. Acta* **1746**, 203–220.
- London, E. and Brown, D. A. (2000). Insolubility of lipids in triton X-100: physical origin and relationship to sphingolipid/cholesterol membrane domains (rafts). *Biochim. Biophys. Acta* **1508**, 182–195.
- Macdonald, J. L. and Pike, L. J. (2005). A simplified method for the preparation of detergent-free lipid rafts. *J. Lipid Res.* **46**, 1061–1067.
- Maeda, Y., Tashima, Y., Houjou, T., Fujita, M., Yoko-o, T., Jigami, Y., Taguchi, R. and Kinoshita, T. (2007). Fatty acid remodeling of GPI-anchored proteins is required for their raft association. *Mol. Biol. Cell* **18**, 1497–1506.
- Makiya, R. and Stigbrand, T. (1992). Placental alkaline phosphatase as the placental IgG receptor. *Clin. Chem.* **38**, 2543–2545.
- Manna, M., Niemelä, M., Tynkkynen, J., Javanainen, M., Kulig, W., Müller, D. J., Rog, T. and Vattulainen, I. (2016). Mechanism of allosteric regulation of beta2-adrenergic receptor by cholesterol. *Elife* **5**, e18432.
- Mayle, K. M., Le, A. M. and Kamei, D. T. (2012). The intracellular trafficking pathway of transferrin. *Biochim. Biophys. Acta* **1820**, 264–281.
- Mayor, S., Presley, J. F. and Maxfield, F. R. (1993). Sorting of membrane components from endosomes and subsequent recycling to the cell surface occurs by a bulk flow process. *J. Cell Biol.* **121**, 1257–1269.
- Mayor, S., Sabharanjak, S. and Maxfield, F. R. (1998). Cholesterol-dependent retention of GPI-anchored proteins in endosomes. *EMBO J.* **17**, 4626–4638.
- Mayor, S., Parton, R. G. and Donaldson, J. G. (2014). Clathrin-independent pathways of endocytosis. *Cold Spring Harb Perspect Biol* **6**, a016758.
- Megha, Bakht, O. and London, E. (2006). Cholesterol precursors stabilize ordinary and ceramide-rich ordered lipid domains (lipid rafts) to different degrees. Implications for the Bloch hypothesis and sterol biosynthesis disorders. *J. Biol. Chem.* **281**, 21903–21913.
- Miaczynska, M. and Stenmark, H. (2008). Mechanisms and functions of endocytosis. *J. Cell Biol.* **180**, 7–11.
- Monnaert, V., Tilloy, S., Bricout, H., Fenart, L., Cecchelli, R. and Monflier, E. (2004). Behavior of alpha-, beta-, and gamma-cyclodextrins and their derivatives on an in vitro model of blood-brain barrier. *J. Pharmacol. Exp. Ther.* **310**, 745–751.
- Mukherjee, S., Soe, T. T. and Maxfield, F. R. (1999). Endocytic sorting of lipid analogues differing solely in the chemistry of their hydrophobic tails. *J. Cell Biol.* **144**, 1271–1284.
- Nes, W. D., Zhou, W., Ganapathy, K., Liu, J., Vatsyayan, R., Chamala, S., Hernandez, K. and Miranda, M. (2009). Sterol 24-C-methyltransferase: an enzymatic target for the disruption of ergosterol biosynthesis and homeostasis in *Cryptococcus neoformans*. *Arch. Biochem. Biophys.* **481**, 210–218.
- Nimmo, M. R. and Cross, N. L. (2003). Structural features of sterols required to inhibit human sperm capacitation. *Biol. Reprod.* **68**, 1308–1317.
- Ohtani, Y., Irie, T., Uekama, K., Fukunaga, K. and Pitha, J. (1989). Differential effects of alpha-, beta- and gamma-cyclodextrins on human erythrocytes. *Eur. J. Biochem.* **186**, 17–22.
- Pang, L., Graziano, M. and Wang, S. (1999). Membrane cholesterol modulates galanin-GalR2 interaction. *Biochemistry* **38**, 12003–12011.
- Parton, R. G., Joggerst, B. and Simons, K. (1994). Regulated internalization of caveolae. *J. Cell Biol.* **127**, 1199–1215.
- Paulick, M. G. and Bertozzi, C. R. (2008). The glycosylphosphatidylinositol anchor: a complex membrane-anchoring structure for proteins. *Biochemistry* **47**, 6991–7000.
- Pike, L. J., Han, X. and Gross, R. W. (2005). Epidermal growth factor receptors are localized to lipid rafts that contain a balance of inner and outer leaflet lipids: a shotgun lipidomics study. *J. Biol. Chem.* **280**, 26796–26804.
- Pucadyil, T. J., Tewary, P., Madhubala, R. and Chattopadhyay, A. (2004). Cholesterol is required for *Leishmania donovani* infection: implications in leishmaniasis. *Mol. Biochem. Parasitol.* **133**, 145–152.
- Refaei, M., Leventis, R. and Silvius, J. R. (2011). Assessment of the roles of ordered lipid microdomains in post-endocytic trafficking of glycosylphosphatidylinositol-anchored proteins in mammalian fibroblasts. *Traffic* **12**, 1012–1024.
- Robinson, M. S. (2015). Forty years of clathrin-coated vesicles. *Traffic* **16**, 1210–1238.
- Rode, M., Berg, T. and Gjøen, T. (1997). Effect of temperature on endocytosis and intracellular transport in the cell line SHK-1 derived from salmon head kidney. *Comp. Biochem. Physiol. a-Physiol.* **117**, 531–537.
- Romanenko, V. G., Davies, P. F. and Levitan, I. (2002). Dual effect of fluid shear stress on volume-regulated anion current in bovine aortic endothelial cells. *Am. J. Physiol. Cell Physiol.* **282**, C708–C718.
- Romanenko, V. G., Rothblat, G. H. and Levitan, I. (2004). Sensitivity of volume-regulated anion current to cholesterol structural analogues. *J. Gen. Physiol.* **123**, 77–87.
- Romanenko, V. G., Roser, K. S., Melvin, J. E. and Begenisich, T. (2009). The role of cell cholesterol and the cytoskeleton in the interaction between IK1 and maxi-K channels. *Am. J. Physiol. Cell Physiol.* **296**, C878–C888.
- Roux, A., Cuvelier, D., Nassoy, P., Prost, J., Bassereau, P. and Goud, B. (2005). Role of curvature and phase transition in lipid sorting and fission of membrane tubules. *EMBO J.* **24**, 1537–1545.
- Samaj, J., Baluska, F., Voigt, B., Schlicht, M., Volkmann, D. and Menzel, D. (2004). Endocytosis, actin cytoskeleton, and signaling. *Plant Physiol.* **135**, 1150–1161.

- Sarnataro, D., Caputo, A., Casanova, P., Puri, C., Paladino, S., Tivodar, S. S., Campana, V., Tacchetti, C. and Zurzolo, C.** (2009). Lipid rafts and clathrin cooperate in the internalization of PrP in epithelial FRT cells. *PLoS ONE* **4**, e5829.
- Schroeder, R., London, E. and Brown, D.** (1994). Interactions between saturated acyl chains confer detergent resistance on lipids and glycosylphosphatidylinositol (GPI)-anchored proteins: GPI-anchored proteins in liposomes and cells show similar behavior. *Proc. Natl. Acad. Sci. USA* **91**, 12130-12134.
- Schroeder, R. J., Ahmed, S. N., Zhu, Y., London, E. and Brown, D. A.** (1998). Cholesterol and sphingolipid enhance the Triton X-100 insolubility of glycosylphosphatidylinositol-anchored proteins by promoting the formation of detergent-insoluble ordered membrane domains. *J. Biol. Chem.* **273**, 1150-1157.
- Shakor, A. B. A., Taniguchi, M., Kitatani, K., Hashimoto, M., Asano, S., Hayashi, A., Nomura, K., Bielawski, J., Bielawska, A., Watanabe, K. et al.** (2011). Sphingomyelin synthase 1-generated sphingomyelin plays an important role in transferrin trafficking and cell proliferation. *J. Biol. Chem.* **286**, 36053-36062.
- Sharma, D. K., Brown, J. C., Choudhury, A., Peterson, T. E., Holicky, E., Marks, D. L., Simari, R., Parton, R. G. and Pagano, R. E.** (2004). Selective stimulation of caveolar endocytosis by glycosphingolipids and cholesterol. *Mol. Biol. Cell* **15**, 3114-3122.
- Silvius, J. R.** (2003). Role of cholesterol in lipid raft formation: lessons from lipid model systems. *Biochim. Biophys. Acta* **1610**, 174-183.
- Singh, A., Mahto, K. K. and Prasad, R.** (2013). Lipidomics and in vitro azole resistance in *Candida albicans*. *OMICS* **17**, 84-93.
- Sorre, B., Callan-Jones, A., Manneville, J.-B., Nassoy, P., Joanny, J.-F., Prost, J., Goud, B. and Bassereau, P.** (2009). Curvature-driven lipid sorting needs proximity to a demixing point and is aided by proteins. *Proc. Natl. Acad. Sci. USA* **106**, 5622-5626.
- Stone, M. B., Shelby, S. A., Nuñez, M. F., Wissner, K. and Veatch, S. L.** (2017). Protein sorting by lipid phase-like domains supports emergent signaling function in B lymphocyte plasma membranes. *Elife* **6**, e19891.
- Subtil, A., Gaidarov, I., Kobylarz, K., Lampson, M. A., Keen, J. H. and McGraw, T. E.** (1999). Acute cholesterol depletion inhibits clathrin-coated pit budding. *Proc. Natl. Acad. Sci. USA* **96**, 6775-6780.
- Tomoda, H., Kishimoto, Y. and Lee, Y. C.** (1989). Temperature effect on endocytosis and exocytosis by rabbit alveolar macrophages. *J. Biol. Chem.* **264**, 15445-15450.
- Veatch, S. L. and Keller, S. L.** (2005). Miscibility phase diagrams of giant vesicles containing sphingomyelin. *Phys. Rev. Lett.* **94**, 148101.
- Wang, T.-Y., Leventis, R. and Silvius, J. R.** (2000). Fluorescence-based evaluation of the partitioning of lipids and lipidated peptides into liquid-ordered lipid microdomains: a model for molecular partitioning into "lipid rafts". *Biophys. J.* **79**, 919-933.
- Wang, J., Megha, and London, E.** (2004). Relationship between sterol/steroid structure and participation in ordered lipid domains (lipid rafts): implications for lipid raft structure and function. *Biochemistry* **43**, 1010-1018.
- Wenz, J. J. and Barrantes, F. J.** (2003). Steroid structural requirements for stabilizing or disrupting lipid domains. *Biochemistry* **42**, 14267-14276.
- Xu, X. and London, E.** (2000). The effect of sterol structure on membrane lipid domains reveals how cholesterol can induce lipid domain formation. *Biochemistry* **39**, 843-849.
- Xu, X., Bittman, R., Duportail, G., Heissler, D., Vilcheze, C. and London, E.** (2001). Effect of the structure of natural sterols and sphingolipids on the formation of ordered sphingolipid/sterol domains (rafts). Comparison of cholesterol to plant, fungal, and disease-associated sterols and comparison of sphingomyelin, cerebrosides, and ceramide. *J. Biol. Chem.* **276**, 33540-33546.
- Xu, Z.-X., Ding, T., Haridas, V., Connolly, F. and Guterman, J. U.** (2009).  $\alpha$ -Avicin D, a plant triterpenoid, induces cell apoptosis by recruitment of Fas and downstream signaling molecules into lipid rafts. *PLoS ONE* **4**, e8532.
- Yamamoto, M., Aizaki, H., Fukasawa, M., Teraoka, T., Miyamura, T., Wakita, T. and Suzuki, T.** (2011). Structural requirements of virion-associated cholesterol for infectivity, buoyant density and apolipoprotein association of hepatitis C virus. *J. Gen. Virol.* **92**, 2082-2087.
- Zidovetzki, R. and Levitan, I.** (2007). Use of cyclodextrins to manipulate plasma membrane cholesterol content: evidence, misconceptions and control strategies. *Biochim. Biophys. Acta* **1768**, 1311-1324.

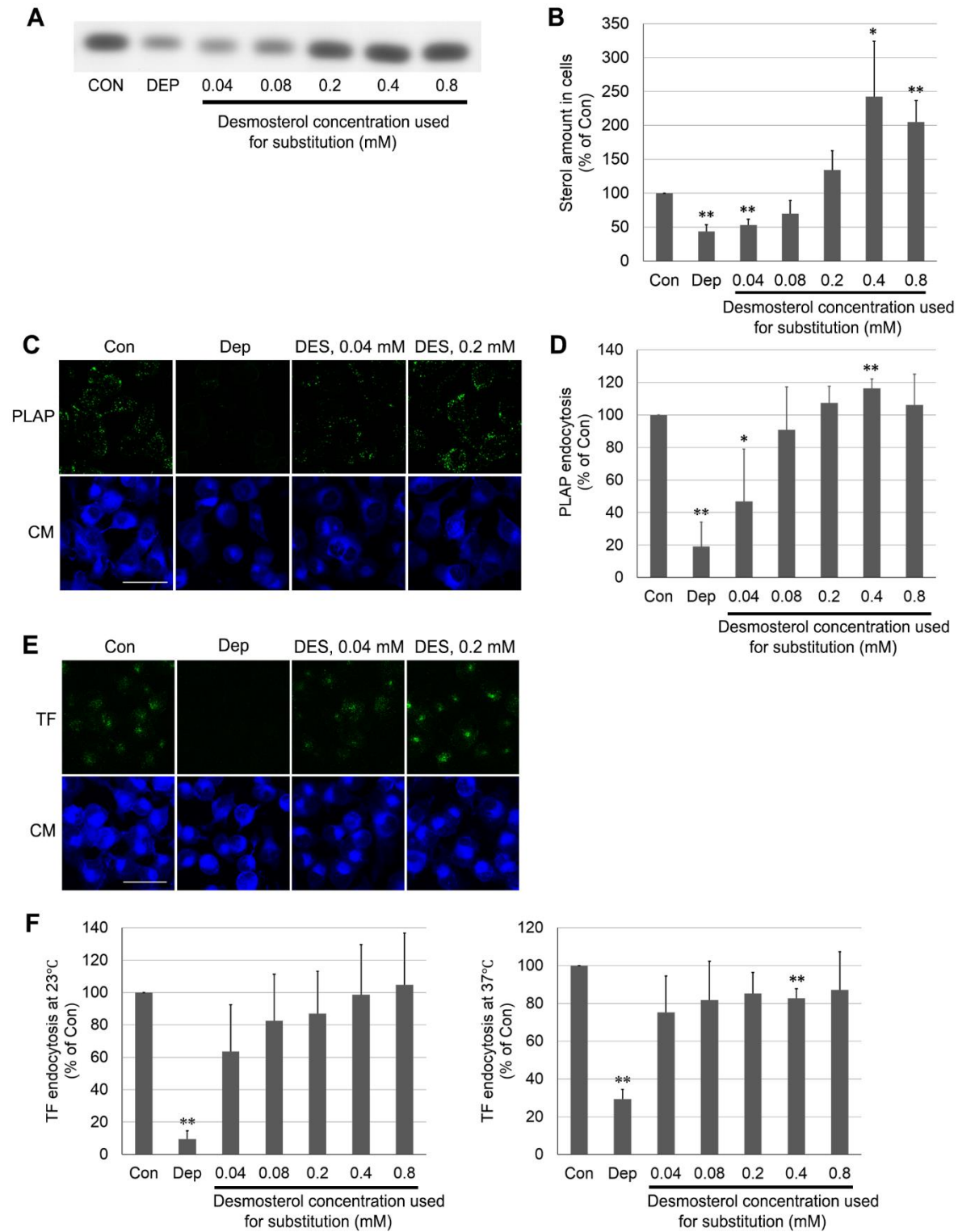


**Fig. S1. Both PLAP- and TF-endocytosis are controlled by the amount of desmosterol. (A)** HP-TLC plate showing cholesterol or mixture of cholesterol and desmosterol amounts in cells

after cholesterol depletion or substitution with desmosterol. (B) Quantified total sterol amounts determined from HP-TLC band intensity. (C) Z-stack micrographs of PLAP endocytosis after cholesterol depletion or substitution with desmosterol. After sterol manipulation in cells, PLAP was clustered with antibody (green fluorescence), and clustered PLAP was internalized by incubation of cells at 37°C for 20 min. Cell surface antibodies were washed off and cell membranes were counter-stained using CellMask (CM, blue fluorescence). (D) Internalized PLAP puncta per cell. In each experiment 3-4 images (total cell number  $\geq 50$ ) were used for puncta quantitation. (E) Z-stack micrographs of TF endocytosis at 23°C after sterol manipulation in cells. After cholesterol depletion or substitution with desmosterol, cells were stained with AF488-TF (green fluorescence), cell surface stain washed off by acid wash and cells were counter-stained with CellMask. (F) TF endocytosis in cells quantitated from integrated green fluorescence intensity (Left: 23°C, right: 37°C). Endocytosis in a total of 50 cells from 2 or more images was analyzed in each sample. In B, D and F, average (mean value) and standard deviation from three independent experiments are shown (i.e.  $n=3$ ). Values normalized to untreated control cells. Con: untreated control cells, Dep: cholesterol depleted cells, DES: desmosterol. Scale bar: 50  $\mu\text{m}$ . \* $P<0.05$ ; \*\* $P<0.01$  compared to 'Con' (unpaired, two-tailed Student's *t*-test).



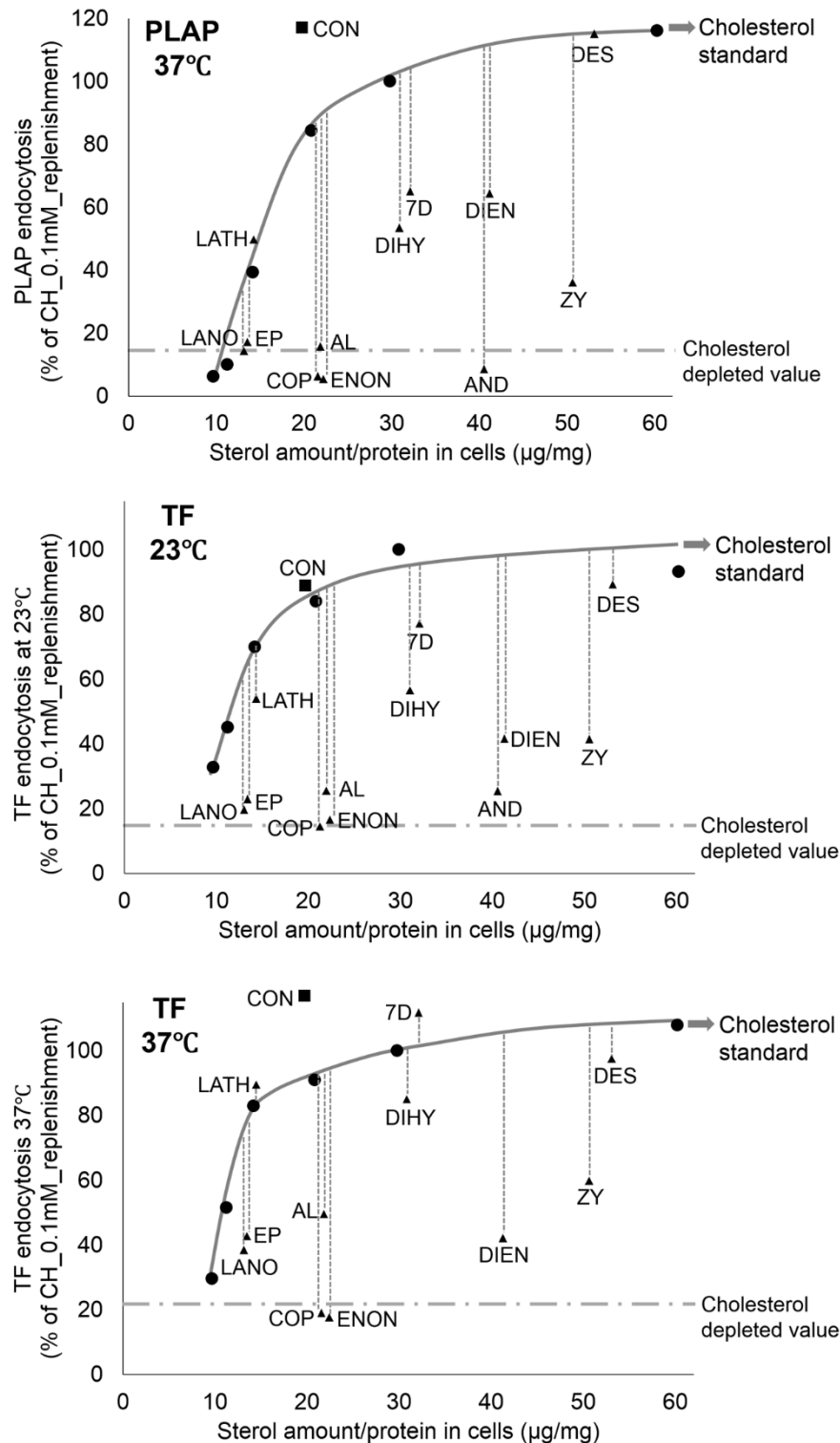


**Fig. S2.** Comparison of endocytosis level for different sterols compared to matching cholesterol levels. (●: cholesterol, ▲: substituted sterol). Gray dotted lines show the difference of endocytosis relative to cholesterol at the same total sterol amount. Dot-dash line shows baseline from cells after cholesterol depletion.

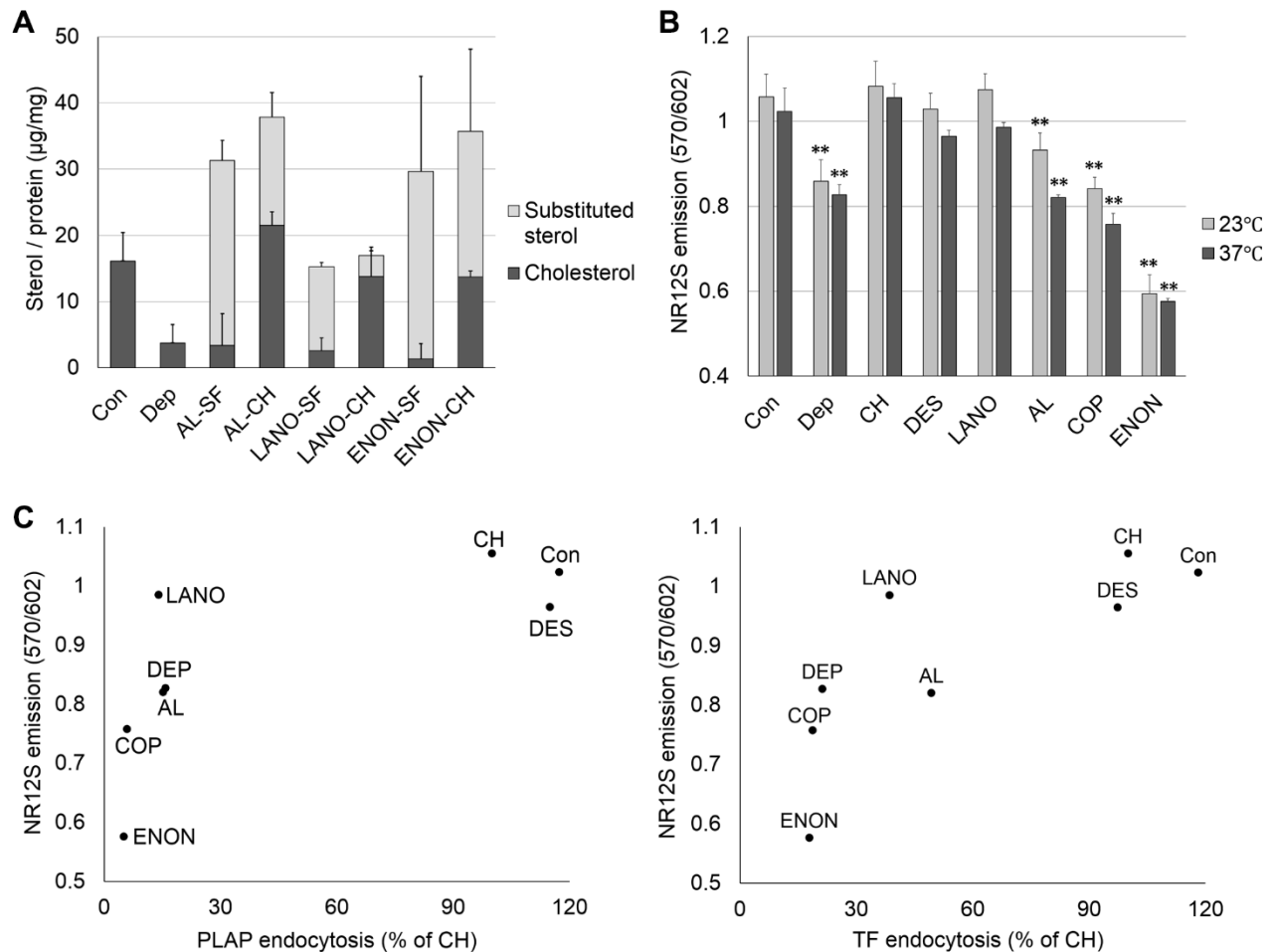


**Fig. S3. Susceptibility of different sterols to removal by a second round of exchange and effect of exchange upon lipid packing.**

(A) The amount of cholesterol and substituted sterol was determined by HP-TLC after cholesterol depletion or sterol substitution followed by a second step of substitution with cholesterol or serum free medium. AL: allocholesterol used in first substitution step, LANO: lanosterol used in first substitution step, ENON: 4-cholesten-3-one used in first substitution step, CH: cholesterol used in second substitution step; SF: serum-free media used in second substitution step control. Average (mean value) and standard deviations are shown ( $n=3$ , except  $n=2$  for AL-SF and AL-CH). (B) NR12S emission ratio (570/602) in sterol-manipulated cells. After cholesterol-depletion or sterol substitution, 40 nM NR12S was added into the cells. The NR12S emission at 570 and 602 nm was measured (excitation at 520 nm) and emission intensity ratio of 570/602 was calculated. Con: untreated control cells, Dep: cholesterol depleted cells; CH: cholesterol replenished cells. Substitutions carried out with: DES: desmosterol, LANO: lanosterol, AL: allocholesterol, COP: coprostanol, ENON: 4-cholesten-3-one. Average (mean value) and standard deviations are shown (i.e.  $n \geq 3$ ). \*\* $P < 0.01$  compared to 'Con' (unpaired, two-tailed Student's  $t$ -test). (C) Average NR12S emission ratio (570/602) vs. average endocytosis level of PLAP (at 37°C) or TF (at 37°C) (see Fig. 3).

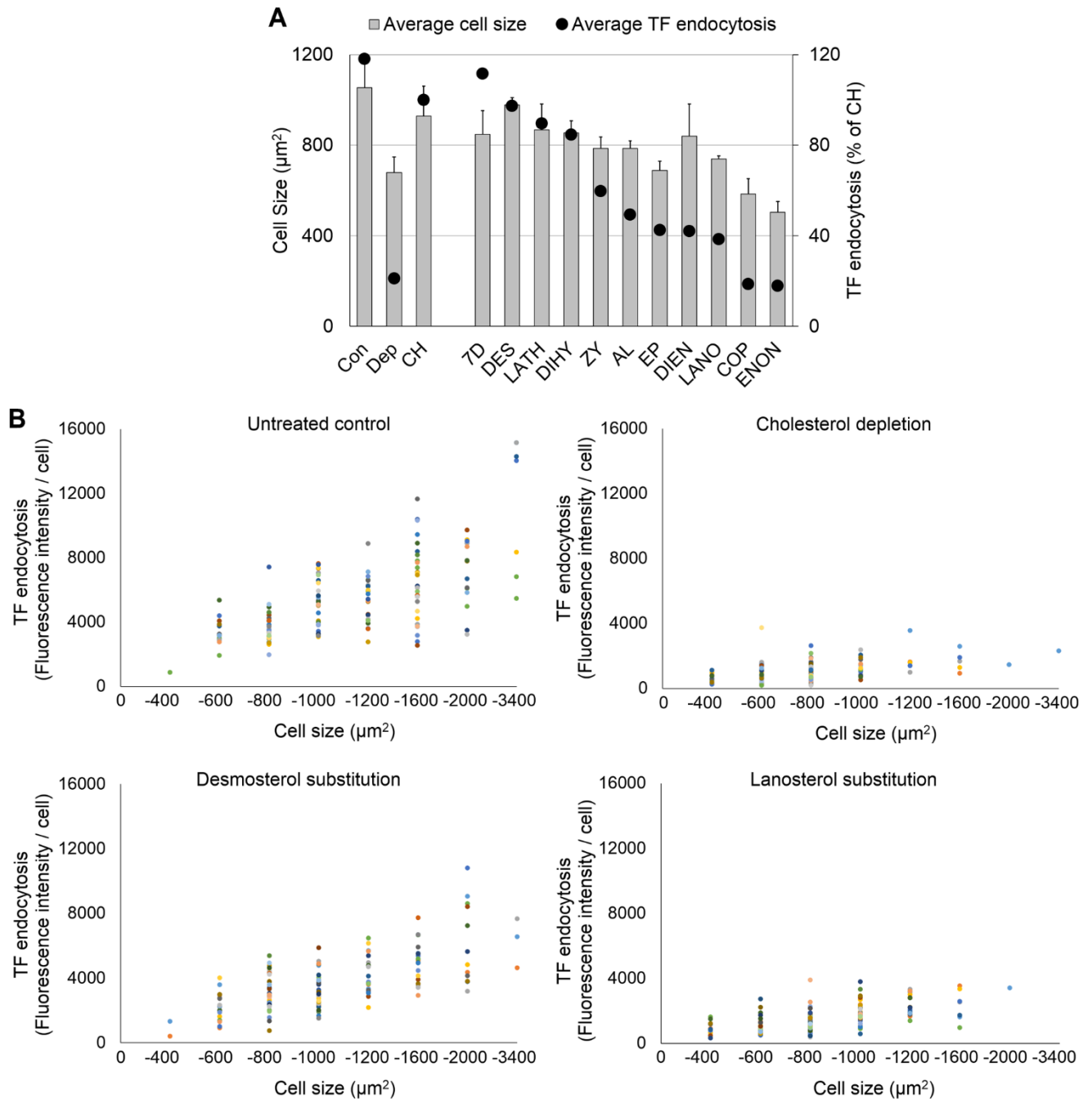


**Fig. S4. Variation in apparent cell size and TF endocytosis.** (A) Average (mean) apparent cell size (as judged by cross-sectional area) and TF endocytosis levels with different sterols. TF endocytosis values are relative to cholesterol-replenished cells. Gray bar: average cell size, black circle: average TF endocytosis. Average (mean value) and (for cell size) standard deviation are shown from independent experiments (see Figure 3D). (B) Graphs showing cell size and TF endocytosis levels for individual cells. Cells were divided into bins of different cell size ranges and AF488-TF fluorescence intensity in each cell is shown.

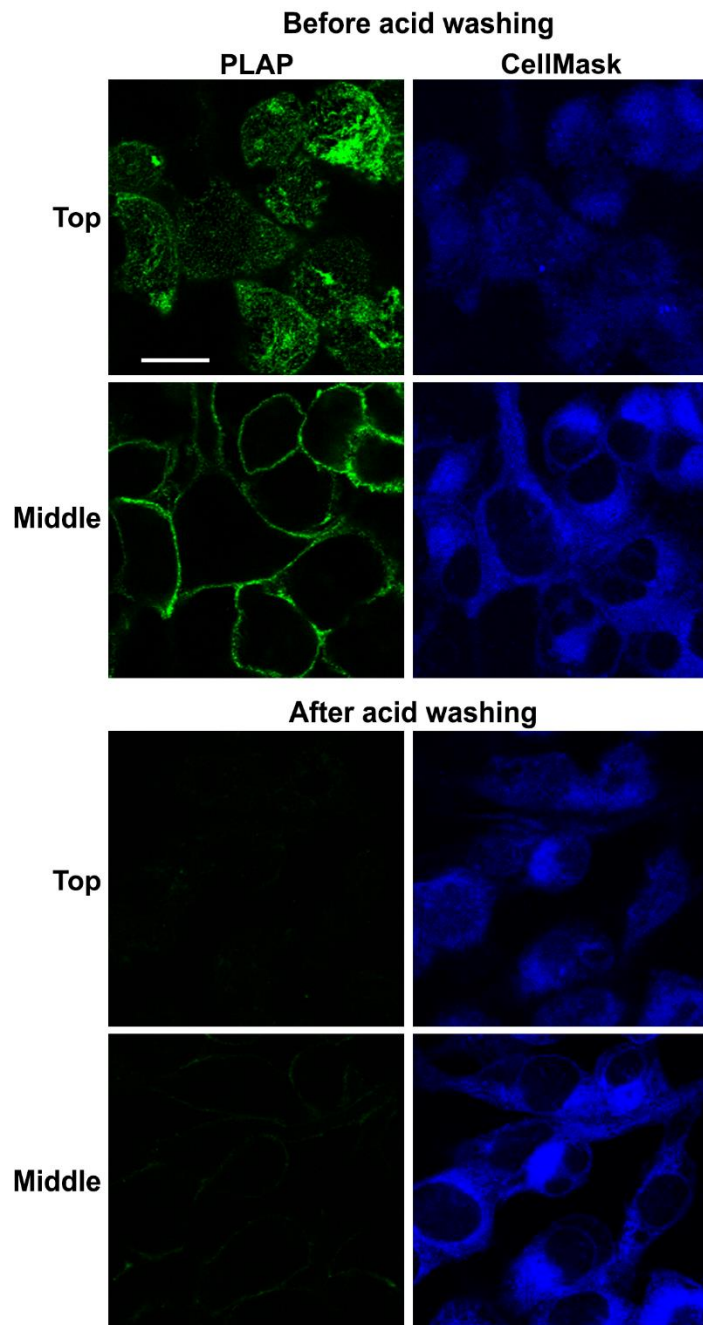


**Fig. S5. Removal of PLAP and fluorescent antibody binding by acid washing.** Images of PLAP immunofluorescence at 4°C (i.e without endocytosis). Upper four panels show cells without acid washing, lower four panels show cells after acid washing. Top refers to confocal sections at the upper surface of the cells. Middle refers to equatorial confocal sections. Scale bar: 20  $\mu$ m.

	i) Raft forming ability			ii) 3 $\beta$ -hydroxyl group		iii) Double bond between 5-6 carbons		iv) Cholesterol tail structure	
	(+++)	(+)	(-)	O	X	O	X	Same	Different
7-Dehydrocholesterol	•			•		•		•	
Cholesterol	•			•		•		•	
Dihydrocholesterol	•			•			•	•	
Epicholesterol	•				•	•		•	
Lathosterol	•			•			•	•	
Desmosterol		•		•		•			•
Allosterol		•		•			•	•	
Choesta-4,6-dien-3-ol		•		•			•	•	
Lanosterol		•		•			•		•
Zymosterol		•		•			•		•
4-cholesten-3-one			•		•		•	•	
Androstenol			•	•		•			•
Coprostanol			•	•			•	•	

**Table S1. Categories dividing sterols depend on the 4 properties.** The sterols were divided into categories according to 4 kinds of properties; i) raft forming ability (Megha et al., 2006; Xu and London, 2000; Wang et al., 2004; Xu et al., 2001; Beattie et al., 2005): raft promoting sterols (+++), intermediate (+), or raft disrupting sterols (-), ii) 3 $\beta$ -hydroxyl group: with (O) or without (X), iii) double bond between position 5-6 carbons: with (O) or without (X), iv) cholesterol tail structure: having same tail structure as cholesterol (same) or different tail structure (different). These properties were analyzed for the relationship with endocytosis efficiency of PLAP and TF.